Recreation in vitro of human intestinal tissue using advanced cell culture technology

GONZALEZ HAU, ARIANA LUCELY

Recreation *in vitro* of human intestinal tissue using advanced cell culture technology

Ariana Lucely Gonzalez Hau

Master of Research

Supervisor: Professor Stefan Przyborski

Department of Biosciences, Durham University

2019

Declaration

This work described herein was carried out in the Department of Biosciences, Durham University between October 2017 and September 2018. All of the work is my own, except otherwise stated. No part has previously been submitted for a degree at this or any other university.

Statement of Copyright

Abstract

The small intestine has the main function of absorbing nutrients and plays a prominent role in the normal function of the body. *In vitro* models have been developed to study the process of molecular transport across the intestinal epithelium as an entry point into the body. This is of particular importance in industry and the ability to perform permeability assays. Conventional intestinal *in vitro* model consists of a single monolayer of epithelial cells, such as the Caco-2 lineage, cultured on a permeable and flat membrane. However, this system has many limitations. It has been demonstrated that the barrier function in the Caco-2 monolayer does not really represent the features of the native small intestinal tissue. Intestinal tissue consists of an integrated system where multiple different cell types interact each other to maintain and perform their function. In this project the effect of coculturing Caco-2 intestinal epithelial cells with fibroblasts was investigated to more closely mimic the structure and function of native tissue and to create a model of the intestinal mucosa. Structural and functional changes were examined during the maturation of Caco-2 cells when they were grown with paracrine factors derived from fibroblasts or in direct co-culture with fibroblasts in a novel 3D cell culture scaffold.

These data indicate that human colon fibroblasts (CCD-18co) and neonatal human dermal fibroblasts (HDFn) produce signals that influenced the Caco-2 barrier structure. It was identified that this change was most likely due to a reduction in junctional complexes between the epithelial cells which are important proteins in the control of paracellular transport. It was demonstrated that this novel 3D intestinal model offers a promising system with greater anatomical and physiological relevance.

Acknowledgements

Firstly, I would like to express my sincere gratitude to my advisor Professor Stefan Przyborski for the continuous support of my MSc study, for his patience, motivation and guidance.

I would also like to thank the laboratory members especially to Nicole Darling, Matthew Freer and Kirsty Goncalves for their very valuable help with cell culturing and kindness during the year. To Dr Mathilde Roger for her help and guidance with the Transmission Electron Microscopy and protein work. I would of course like to thank Lydia Costello, Lucy Smith, Henry Hoyle, Benjamin Allcock, Amy Simpson, Steven Bradbury, Craig Manning, Rebecca Quelch, Felicity Liu and Claire Mobbs for popping in to help during lab work. To Dr Gioconda Moura for being such a lovely person and all her invaluable support on bad days and when not everything went to plan.

I must express my very profound gratitude to my parents, my sisters and my boyfriend whom, despite the distance, were always there putting their best effort so that I was well. Also, for their continuous encouragement through the process of researching and writing this thesis.

Finally, I would like to acknowledge Consejo Nacional de Ciencia y Tecnología (CONACyT) and Secretaría de Investigación, Innovación y Educación Superior (SIIES) whom without their funding this project would not have been carried out.

TABLE OF CONTENTS

LIST OF FIGURES

LIST OF TABLES

Abbreviations

xg – Relative Centrifugal Force

AJ – Adherens Junction

Caco-2 – Human Colorectal Adenocarcinoma Cell Line

CCD-18co – Human Colon Normal Fibroblasts

cDNA – Complementary Deoxyribonucleic Acid

Ct – Cycle Threshold

DMEM – Dulbecco's Modified Eagle Medium

ECM – Extracellular Matrix

FBS – Foetal Bovine Serum

GIT – Gastrointestinal tract

HDFn – Human Dermal Fibroblasts, neonatal

JAM – Junctional Adhesion Molecules

kPa – Kilo Pascal

LPM – Lateral Plasma Membrane

L-pNIPAM – Poly(N-isoporpylacrylamide) modified

MEM – Minimal Essential Medium

mRNA – Messenger Ribonucleic Acid

OCT – Optimal Cutting Temperature compound

PBS – Phosphate Buffered Saline

PFA – Paraformaldehyde

qPCR – Quantitative Polymerase Chain Reaction

RLT – RNeasy Lysis Buffer

rpm – Revolutions per minute

RT – Reverse Transcription

SDS-PAGE – Sodium dodecyl sulfate polyacrylamide gel electrophoresis

SEM – Standard Error of the Mean

TBST – Tris Buffered Saline and Tween 20

TEM – Transmission Electron Microscopy

TEER – Trans Epithelial Electrical Resistance

TJ – Tight Junction

1. Introduction

1.1. Intestine Anatomy and Physiology

The digestion and absorption of nutrients and water are the function of the intestines. They form part of the gastrointestinal tract (GIT) that consists of connected muscular tube lined by mucous membrane, facilitating the digestive process, starting from the oral cavity, continuing through the pharynx, oesophagus, stomach, small intestine, large intestine and finalizing to the rectum and anus. The digestion process occurs by the action of muscles contractions and enzymes (Young, O'Dowd, & Philip, 2014). Although the organs in the GIT have differences in structure and function, they have four distinct functional layers. The outermost layer is the adventitia, also known as serosa, that consists of mesothelium, epithelium and underlying connective tissue. The second layer is muscularis propria which consists of thick layers of smooth muscle. Then is placed the submucosa layer of loose collagenous connective tissue and this is where blood vessels, lymphatic vessels and nerves plexuses are found. The inner layer, the most close to the lumen, is the mucosa (figure 1) which consists of three components: the epithelium for excretion and absorption, a supporting lamina propria and the muscularis mucosae which provides local movement (Ross *et al*., 1995; Young *et al*., 2014). The small intestine is the primary organ of the GIT and is where most of the digestion and absorption occurs. The first part of the small intestine is the duodenum, receiving partly digested food and acid from the stomach. The second part is the jejunum where occurs the absorption of sugar, amino acids, and fatty acids. The last part of the small intestine is the ileum and is where residual nutrients from the jejunum are absorbed (Collins & Bhimji, 2017). The small intestine is lined, in the lumen side, with structures called villi. Each villus is composed of different types of epithelial cells: intestinal stem cells with the function to continually renewed the intestinal mucosa; absorptive enterocytes; goblet cells producing and secreting mucins to maintain the protective mucus barrier; entero-endocrine cells that provide peptide hormones; and Paneth cells which are the responsible of producing and secreting antimicrobial peptides during the innate mucosal defence (Patton & Thibodeau, 2013). In the luminal side of the epithelial cells it is found small finger-like protrusions called microvilli which are designed to increase the surface area of the membrane, maximising the absorption of nutrients (Collins & Bhimji, 2017; Young *et al*., 2014).

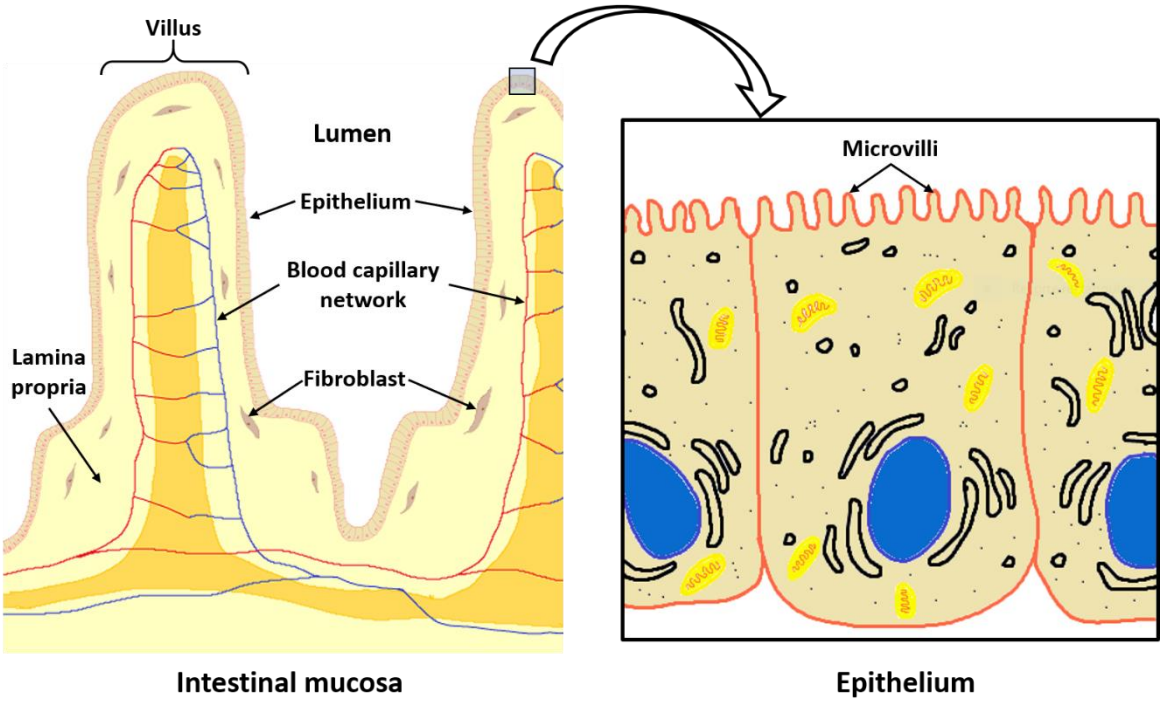

Figure 1: Schematic representation of small intestine mucosa layers.

1.2. Junctional complexes

The epithelium is composed of layers of cells that are closely attached each other. The development of direct cell-cell contact is regulated by the interaction of specialised junctional protein complexes localized along their lateral membranes. Junctional complexes consist of three adhesive structures: 1) Tight junctions (TJs), localised at the uppermost zone close to the apical side of the cells. 2) Adherens junctions (AJs), which are in the middle position just below the TJs. 3) Desmosomes localised at the bottom position (figure 2). Those three components are mainly distributed in the apical side, regulating the epithelial barrier function (Ebnet, 2008).

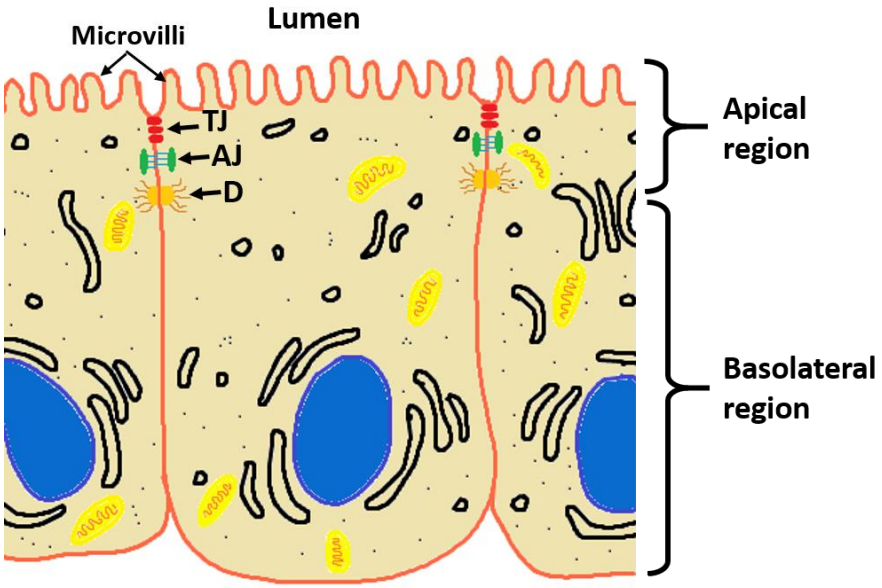

Figure 2: Schematic representation of junctional complexes localization in epithelial cells. Tight junctions, adherens junctions and desmosomes conform the junctional complexes and they are mainly localised in the apical region of epithelial cells, with the role of regulate cell permeability, adhesion of neighbouring cells and maintain tissue cohesion, respectively. TJ, tight junctions; AJ, adherens junctions; D, desmosomes.

1.2.1. Tight Junctions

The first junctional complex structure, tight junctions (TJs), present different functions, the most of which are in the homeostasis of epithelial integrity and transport. Moreover, they are also important in the regulation of cytoskeleton, cell proliferation and differentiation. These junctional proteins tightly connect adjacent epithelial cells to each other forming an intramembrane barrier (represented in figure 3) and therefore regulate the permeability of solutes and ions through the paracellular pathway. Tight junction complexes are physically found in the apical side of the epithelial cells and are composed of more than 40 specialised proteins. These include transmembrane proteins and cytosolic proteins that link the junctional membrane to the cytoskeleton (Yamazaki *et al*., 2008).

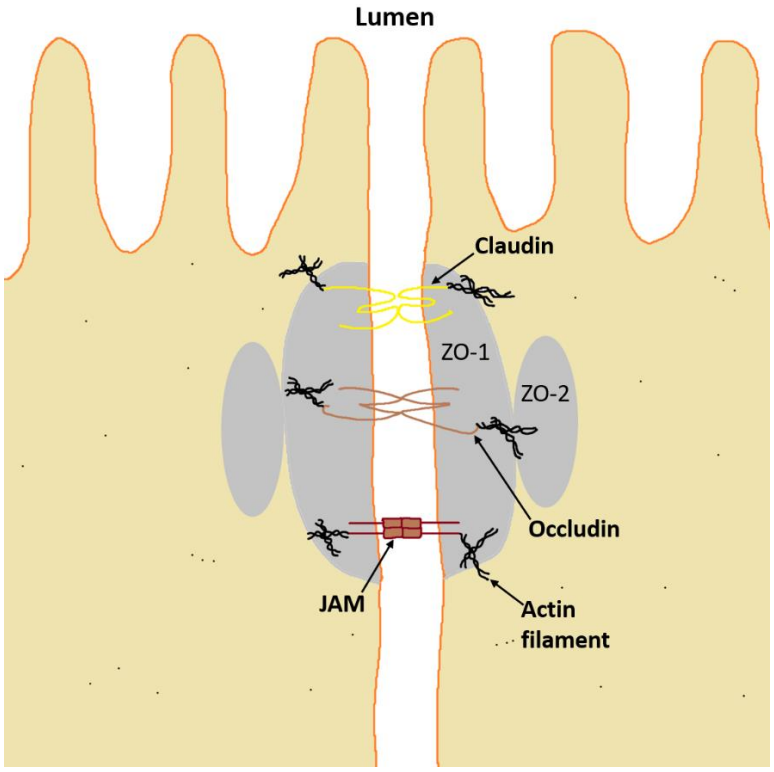

Figure 3: Schematic representation of tight junction structures in epithelial cells. TJs are composed of transmembrane proteins, including claudins, occludins, and junctional adhesion molecules (JAM), which interact with cytoplasmatic adaptor proteins as zonula occludens proteins (ZO-1 and ZO-2) that often interact with actin filaments. Those proteins interact in a coordinated manner to form the intestinal barriers.

The main proteins that are found in the transmembrane strands are MARVEL domain proteins (in which occludins and tricellulin are included), claudins and junctional adhesion molecules (JAMs) (Zihni *et al*., 2016). Moreover, the cytoskeleton is composed of a complex protein network. Zonula occludens 1 (ZO-1) is one of the cytoskeletal adaptor proteins found to be associated with TJs (Zihni *et al*., 2016). ZO-1 protein also participates in the tensile force acting on adherens junctions and act as the major cytoskeletal organizer in epithelial cells (Tornavaca *et al*., 2015).

It is well known that TJ regulate cell behaviour through different molecular signalling mechanisms. Tight junction transmembrane proteins interact with a complex cytoplasmic protein network. In this complex can be found several different scaffold proteins that perform critical roles bringing together two or more proteins to facilitate their interactions (Zihni *et al*., 2016). Those scaffold proteins are involved in the communication and control of cell-cell tension, angiogenesis, barrier formation, proliferation and cell size regulation (González-Mariscal *et al*., 2017; Tornavaca *et al*., 2015). As described previously, ZO-1 is a peripherally associated scaffolding protein that couples transmembrane proteins of the claudin and JAM families to cytoplasmatic proteins and to actin

filaments. Thus, it leads to a rearrangement of the actomyosin cytoskeleton and therefore controls the cell shape.

1.2.2. Adherens junctions

Adherens junctions are the second structures that are an integral part of the junctional complexes. During the epithelial cell differentiation, they are the responsible to initiate and regulate the cell-cell belt connection. E-Cadherin is the major adhesion proteins of AJs which, altogether with nectins, initiate the adhesion of neighbouring epithelia cells (Zihni *et al*., 2016). This trans-cadherin interaction between adjacent cells leads to the recruitment of tight junction components ZO-1 and JAM. At the cytoplasmic region, E-cadherin tails interact with catenin proteins, forming a multiprotein complex that generate a transcellular network of actin filaments (Ebnet, 2008; Hartsock & Nelson, 2008).

1.2.3. Desmosomes

Desmosomes are localised below the adherens junctions on the lateral cell membrane. These junctions have the main function of maintaining the integrity of the tissue when exposed to mechanical stress. They are presented as multiprotein complexes that mediate the adhesion between adjacent cells at multiple sites along the lateral membranes. Those adhesive interactions are associated with the intermediate filament cytoskeleton which enable them to maintain the tissue cohesion (Kowalczyc *et al*., 2013).

1.3. Current intestinal models

1.3.1. Intestinal animal models

Drug development in the pharmaceutical industry entails high costs and high rates of clinical failures during the preclinical screens that are bottleneck in the process. The use of animal models in the industry for testing novel drugs is common as it is necessary to have large-scale animal testing in the development of new drugs (Edmondson *et al*., 2014). Moreover, the use of animal models raises the costs of testing drug compounds as additional funds must be expected to care for animal maintenance and the infrastructure required for effected animal husbandry (Ziegler *et al*., 2016). In addition, it has been reported that nearly 10% of drugs fail the first clinical phase that is the most expensive phase of clinical trials (Hay *et al*., 2014). This is because the current models may not predict how human tissue will react. For that reason, it is important to optimize the first steps in the

development of new drugs, using more physiologically relevant *in vitro* models to predict native tissue interactions before the clinical phases.

In vitro cell-based assays have been adopted as a gold standard industrial practice over the last few decades as tools to predict cellular responses in human tissue such as the modelling of in vivo permeability, metabolism, distribution and excretion (Khanna, 2012). The benefits of simple cell based assays are that they can be performed under controlled conditions and can be monitored with advanced microscopy (Nierode *et al*., 2015). Additionally, the use of well characterised transformed cell lines allows for the replication of results industry wide, reducing lab to lab differences. In comparison with the use of animal models, cell-based assays provide simple, cost and time-effective practices. As such, more advanced cell-based models which take the advantages of the utilisation of cheap, well characterised cell lines combines with more relevant 3D model geometry and multiple cell populations can be a powerful tool, reducing the need for animal testing, solving the issue of standardisation when using *ex vivo* models and adopting the principles of the 3Rs (Replacement, Reduction and Refinement).

1.3.2. *In vitro* intestinal tissue models

To date, most of the *in vitro* models that are being used for novel drug tests are based on simple 2D monolayer models. Human epithelial Caco-2 is the gold standard cell line used in drug testing due to their potential to differentiate into functional enterocytes and grow in a monolayer. The intestinal mucosa is comprised of an epithelial layer, an underlying lamina propria and the muscularis mucosa. The presence of microvilli in the intestinal mucosa is essential as they are the functional unit for nutrient absorption. Caco-2 cells are derived from a human colonic adenocarcinoma and it has been widely used for the prediction of intestinal absorption of drug candidates (Kauffman *et al*., 2013; Waltenberger *et al*., 2008). Even though, this cell line originates from colon carcinoma. Under normal cell culture conditions, they spontaneously differentiate into mature cells, developing microvilli and tight junction complexes, characteristics found in real intestine tissue. Moreover, their easy culture maintenance and scalability, make them a feasible candidate to use for cell-based assays in novel drug development.

Caco-2 monolayer model

Most laboratories have adopted the use of Caco-2 cells to better reproduce the intestinal mucosa. These cells are cultured on a semipermeable membrane, allowing the exchange of ions, nutrients

and waste across the monolayer. Caco-2 cells reach confluency within 3 days with a seeding density of 10^5 cells/cm^2 and then they reach the stationary phase after 10 days of being in culture. Transport studies are usually done after 3 weeks of culture because it is when differentiation is completed (Braun *et al*., 2000). Transepithelial electrical resistance (TEER) is measured in order to monitor the monolayer integrity. TEER value change in dependence of the growth phase. They reach higher values at differentiation stage demonstrating their barrier function (Borchardt 1989).

There are some factors that influence Caco-2 behaviour. It has been reported that the number of passages can influence metabolic activities. Zafarvahedian & Ghahremani (2018) observed that Caco-2 cells in the passage number range of 5-15 there is a higher insulin-degrading enzyme activity compared to higher passage number ranges. Moreover, TEER values are also affected in dependence of the passage number. When Caco-2 cells are used in later passages, TEER values from the monolayer has been shown to increase. This differences in the cellular behaviour may be due to the cell population heterogeneity that Caco-2 presents (Briske-anderson *et al*., 1997). Seeding density is another factor that affects the time until cell differentiation as cells reach this phase when they are confluent. It seems to have a negative effect on the monolayer formation and therefore TEER values may increase (Behrens & Kissel, 2003). Medium composition can also influence Caco-2 cells growth. Growth factors like glutamine has been reported to have an important effect on the synthesis of tight junctions proteins (Li *et al*., 2004). In addition, changes in the pH found in the medium disturbs internal Caco-2 cell pH. It has been reported that pH 7.2 induces Caco-2 cells proliferation while alkalinity promotes cell differentiation (Perdikis *et al*., 1998). These variables affecting Caco-2 behaviour reported above highlight the inherent variability in Caco-2 models. Thus, there is a need to monitor the culture characteristics during growth and differentiation under specific experimental conditions.

1.3.3. 3D *in vitro* intestinal tissue models

New improved 3D models have been developed in order to satisfy needs found in the conventional monolayer model. Recently, it has been reported that 3D intestinal *in vitro* models better simulate the structure and function of native tissue compared than their 2D counterparts (Li *et al*., 2013; Matsusaki *et al*., 2015; Pereira *et al*., 2015). These results are leading tissue engineers to move into a new design approach of cell culture that better mimic real tissue microenvironment.

Many 3D intestinal models developed are based in the co-culture of Caco-2 with different cell lines. The addition of other cell types such as fibroblasts, immune cells and goblet cells is increasingly

being more popular. This is due to the searching for improvements in the epithelial cells function. The use of fibroblasts in co-culture with Caco-2 cell line is important for the constant maintenance of the microenvironment. As mentioned previously, the intestinal mucosa is composed of underlying mucosa, also called lamina propria, that provides extracellular matrix (ECM) components, as collagens, fibronectin, fibrin, and growth factors that have a critical signalling role and enhance epithelial cells proliferation (Elamin *et al*., 2012). Two interesting fibroblast cell lines that has shown favourable results when they are used in intestinal models are Human colon normal fibroblasts (CCD-18co) and neonatal Human dermal fibroblasts (HDFn). CCD-18co fibroblast has been demonstrated to be a good candidate cell line to be simultaneously cultured with Caco-2 cells (Gèoke *et al*., 1998; Pereira *et al*., 2015). This cell line was isolated from human normal colon tissue. Previous work has developed a 3D model of intestinal tissue with both cell lines in co-culture, demonstrating that CCD-18co cells are able to remodel the matrix producing extracellular matrix components that enhance Caco-2 proliferation (Pereira *et al*., 2015). ECM components are important for organization, structure and support of tissues, and cell communication. Neonatal Human Dermal Fibroblast (HDFn) cells play a critical role in the normal wound healing. This dermal fibroblast line has previously been widely used to reconstruct skin tissue models due to their ability to produce collagen and elastic fibres (Elamin *et al*., 2012). Taking this into account, researchers has begun to use this cell line to enhance Caco-2 proliferation in intestinal models (Matsusaki *et al*., 2015). Thus, *in vitro* co-culture of epithelial cells with fibroblasts is essential to promote cell proliferation and therefore to simulate the microenvironment of real tissue.

In vitro spheroid culture is an option for 3D culture over monolayer models. In this 3D culture system, the cells are grown into aggregates or spheroids on matrix, embedded within a matrix or in suspension. This system provides a microenvironment where two different cell lines could be in co-culture in a 3D system. Some intestinal spheroid models have been developed, to study the Caco-2 cell line drug or stress responses, using natural materials as scaffold (Elamin *et al*., 2012; Hoffmann *et al*., 2015). However, content variation in the substrate could be presented as they are prepared in batch and materials may interfere with cell behaviour.

1.3.4. Intestinal organoids

Recently, there has been significant progress in organoid culture to model the intestinal tissue. This recent development is also being considered as a 3D culture system. This novel culture systems consists on the culture of primary tissue cultures that can be maintained long term within a complex

extracellular matrix using Matrigel® recapitulating the physiology, the 3D architecture, the genetic signature of the native tissue and their tissue regeneration capability (Nakamura 2018). Until recently, it has been reported three sources of intestinal organoids: self-organizing pluripotent stem cells (PSCs), intestinal adult stem cells (ASCs) or generated by a transcription-factor-mediated direct lineage reprogramming of fibroblasts (Jung *et al*., 2011; Miura & Suzuki, 2017; Spence *et al*., 2011). There are studies that show intestinal organoids developing structures like crypts and villi that resemble native tissue. Moreover, Zachos *et al*., (2016) reported that they also exhibit *in vivo*-like functions like mucus production, absorptive function and secretory function.

Although the advantages of the use of intestinal organoids to recreate *in vitro* intestinal tissue, the nature of their structure involve certain challenges. Existing bioengineered sensors that are widely used to monitor conventional 2D intestinal models are not compatible for this novel system *(Kim et al*., 2018). Furthermore, it is found other difficulties with imaging and co-culturing with other cell types (Richmond & Breault, 2018). There is a need to develop new technologies or to adapt existing ones to allow analysis and monitoring of intestinal organoids models.

1.4. Conditioned medium co-culture

An alternative to the direct co-culture and often preferred co-culture system is the use of conditioned media to facilitate maturation of cells. Conditioned media consists of a reservoir of secreted proteins that act as mediators in the cell-cell interactions. These interactions include the regulation of in the morphology, proliferation, adhesion and polarization of epithelial cells. Examples of those mediators might be growth factors, enzymes and extracellular matrix components (ECM) (Dowling & Clynes, 2011). The use of the cell secretome is often preferred in cell culturing due to the feasibility in the manual labour as in one single batch, it possible to feed a considerable number of single cultures. At an optimized concentration, conditioned media can maintain cells structure and function to levels similar to those in direct co-culture of the two cell lines of interest (Jeong *et al*., 2016) whilst limiting batch variance by pooling conditioned media before use.

1.5. Alvetex® 3D cell culture technology

3D scaffolds for cell-based assays better mimic the morphology and behaviour of *in vivo* tissue. It is well known that the physical microenvironment has a main role in the cell differentiation. Popularly, 2D models has been used in cell-based assays, however when epithelial cells are differentiated they

develop a flattened structure (Edmondson *et al*., 2014). In contrast, it has been observed that when they are set up in a 3D substrate or scaffold, epithelial cells can acquire a more *in vivo*-like morphology and physiology (Sung *et al*., 2011).

Different options of 3D technology can be chosen and adapted according to the necessities and biocompatibility of the tissue model being developed. In some models it has been physical scaffolds that provides a cell-friendly environment and support 3D cell culture. Scaffolds could be made of synthetic or natural materials (Knight & Przyborski, 2015; Yu *et al*., 2012). Traditionally, 3D models are based in the use of substrates made of relatively short shelf life natural materials such as collagen and Matrigel®. Scaffolds made of natural materials may allow the cells to produce metabolites that consequently can influence cell behaviour in non-controllable ways. Therefore, it has its issues when a study of cell behaviour and interactions is intended. This in part has led to the design of new *in vitro* 3D models based on the use of synthetic material scaffolds. Dosh *et al*. (2017) evaluated three intestinal models using hydrogel scaffolds. The use of a novel synthetic non-biodegrable hydrogel, L-pNIPAM, enhanced epithelial cells to develop villus-like structures. However, these substrates do not permit homogeneous cell growth and efficient mass transfer of gas and nutrients throughout the material. In addition, Matsusaki *et al*. (2015) designed a '3D co-culture model' consisting of layers of HDFn fibroblasts co-cultured with a monolayer of Caco-2 on a synthetic membrane. As it was stated previously, this co-culture system has its advantages and fibroblasts modulate epithelial cell maturation. However, this model is based on the use of a flat semipermeable membrane that does not provide the cells the physical support to develop their *in vivo*-like morphology.

AN alternative synthetic scaffold, Alvetex®, has been developed for 3D technology that consists of a highly porous polystyrene material designed to enable robust and reproducible 3D cell culture more closely representing the *in vivo* microenvironment (Maltman & Przyborski, 2010).

Alvetex® is engineered into a 200 μm thick membrane with pore sizes of 36-40 μm (figure 4). This allows the cells to receive adequate diffusion of nutrients within the scaffold and the exchange of gas and waste products. Cells grow and attach within the Alvetex® membrane and acquire *in vivo*-like 3D morphologies (Maltman & Przyborski, 2010). Consequently, researchers at Durham University have begun to design intestinal mucosal models using Alvetex® cell culture technology.

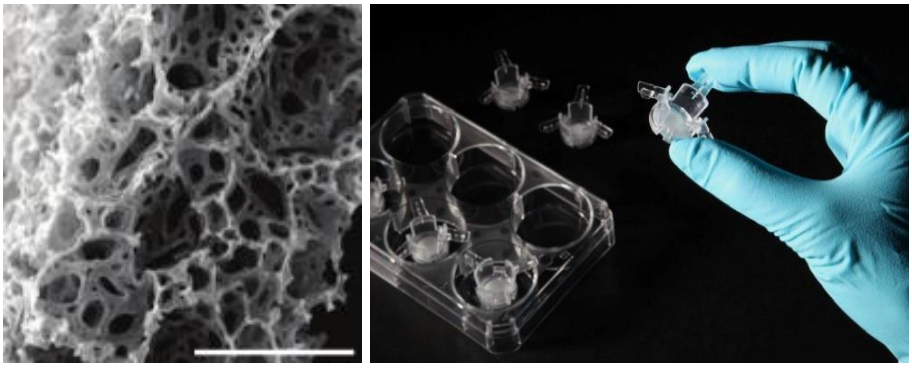

Figure 4: Alvetex technology for 3D cell culture. Alvetex is a synthetic scaffold composed of 200 µm thick of highly porous polystyrene that enable the cells to acquire tissue-like structures. At the left, scanning electron micrograph of Alvetex®, scale bar 100 µm. At the right, the 12 well format of Alvetex® Scaffold. Taken from reinnervate.com.

1.6. Aims and objectives

It is well known that the configuration of the microenvironment is important for the maturation and differentiation of cells in *in vitro* cultures. 3D microenvironment and paracrine signalling between cells types found in the intestinal mucosa are important factors that influence the development of models that more closely represent native intestinal tissue.

First, it was hypothesised that culturing Caco-2 cells in co-culture with fibroblast cell lines would enable epithelial cells to develop more representative lateral barriers. Secondly, it was also hypothesised that the three-dimensional environment would enhance epithelial cells phenotype. For these reasons, the aim of this project is to characterise the expression and distribution of junctional complexes proteins in *in vitro* 2D and 3D intestinal tissue models and compare their changes in expression with the real tissue. The main objectives of the project are:

- To compare the structure of epithelial lateral membranes acquired when Caco-2 epithelial cells are cultured in 2D and 3D microenvironment.
- To compare the results in structural lateral membrane changes with the human intestinal tissue.
- To study the paracrine effect of two cell lines of fibroblasts: CCD-18co and HDFn, in the structure and integrity of the lateral membrane barrier in Caco-2 epithelial cell line.
- To compare changes in the expression of junctional complexes proteins in 2D models when Caco-2 cells are paracrine regulated by two fibroblast cell lines and untreated Caco-2 cells.

- To compare changes in the gene and protein expression of junctional complexes in 3D and 2D models with control.

2. Materials and Methods

2.1. 2D cell culture

Human colorectal adenocarcinoma cell line (Caco-2)

Caco-2 cells (ECACC) were cultured in medium DMEM (Gibco, ThermoFisher) supplemented with 10% Fetal Bovine Serum (Gibco, ThermoFisher), 2 mM L-Glutamine (Gibco, ThermoFisher) and 50,000 U Penicillin-Streptomycin (Gibco, ThermoFisher). Following instructions from supplier, culture was kept until a confluence of around 70% and flasks were kept in a humidified atmosphere with 5% CO_2 at 37°C. Media was change every 2-3 days. Cells were frozen down in 1 mL cryovial (ThermoFisher) at $2x10^6$ cell/mL in 1mL 5% DMSO and 95% DMEM and they were kept at -150°C.

Human dermal fibroblasts, neonatal (HDFn)

HDFn cells (Life Technology) were cultured in DMEM (Gibco, ThermoFisher) supplemented with 10% Fetal Bovine Serum (Gibco, ThermoFisher), 2 mM L-Glutamine (Gibco, ThermoFisher) and 50,000 U Penicillin-Streptomycin (Gibco, ThermoFisher). Cells were kept in culture in a humidified atmosphere with 5% CO_2 at 37°C until around 70% of confluence, changing the media three times a week. Cells were frozen down in 1 mL cryovial (ThermoFisher) at $2x10^6$ cell/mL in 1mL 5% DMSO and 95% DMEM and they were kept at -150°C.

Human colon normal fibroblasts (CCD-18co)

CCD-18co (ATCC) were cultured in MEM (Gibco, ThermoFisher) supplemented with 10% Fetal Bovine Serum (Gibco, ThermoFisher), 1 mM Sodium Pyruvate (Gibco, ThermoFisher), 2 mM L-Glutamine (Gibco, ThermoFisher) and 50,000 U Penicillin-Streptomycin (Gibco, ThermoFisher). Cells were kept in culture in a humidified atmosphere with 5% CO_2 at 37°C until around 70% of confluence, changing the media every 2 days. Cells were frozen down in 1 mL cryovial (ThermoFisher) at $2x10^6$ cell/mL in 1mL 5% DMSO and 95% MEM and they were kept at -150°C.

Paracrine signalling models

Transwell® polycarbonate membrane cell culture 12 mm inserts (Sigma-Aldrich) were pre-treated by soaking them in 70% ethanol for 5 minutes. Then they were washed in PBS for 5 minutes and washed in PBS for 1 minute. The inserts were transferred to a 12 well cell culture plate (Greiner bio-one) and 1.5 mL of DMEM supplemented media was added to the outer part of the membrane until required.

Caco-2 cells from passages 49 to 55 were used to construct the models. 250,000 cells were seeded by homogenous dropping 100 µL of cell suspension throughout each insert. They were incubated in a humidified atmosphere with 5% CO_2 at 37°C for at least 2 h. Then, 750 mL of DMEM supplemented media was added to the inner part of the membrane and the plate was returned to the incubator until two days.

From the second day of culture, conditioned media was used to feed the models every two days until 21 days when Caco-2 cells are differentiated. A schematic protocol of the culture is presented in the figure 5. To prepare the conditioned media, fibroblasts were cultured in flasks to become confluent. Media from no more than 48h in culture was centrifuged at 200 xg for 3 min and the supernatant was mixed up in a proportion 1:1 with fresh DMEM media.

For the control 2D model, Caco-2 cells were fed every two days with complete DMEM media until differentiation at the 21st day of culture.

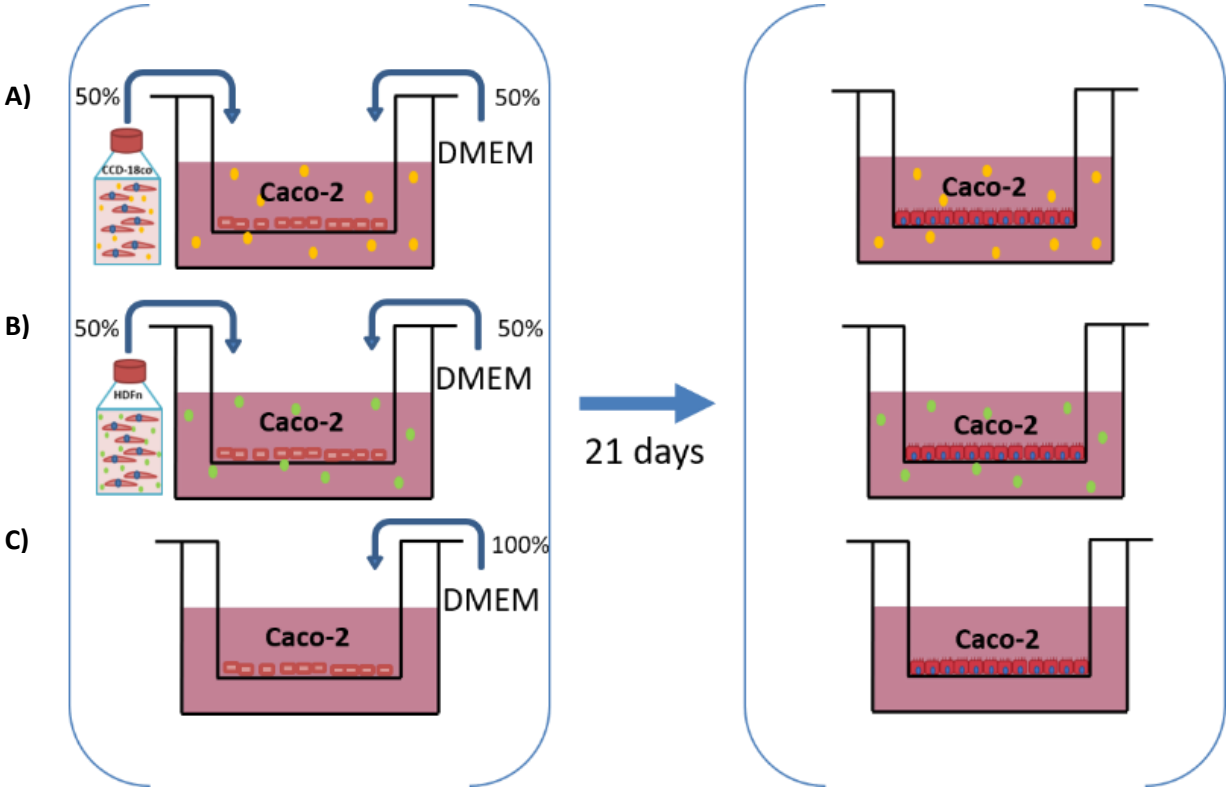

Figure 5: Schematic protocol of 2D models culture. A) 2D CCD-18co: Caco-2 cells cultured in Transwell® inserts and maintained with CCD-18co cells conditioned media until differentiation; B) 2D HDFn: Caco-2 cells cultured in Transwell® inserts and maintained with HDFn cells conditioned media until differentiation; and C) Control: Caco-2 cells cultured in Transwell® inserts and maintained with DMEM.

2.2. 3D cell culture

Alvetex® polystyrene scaffolds, in their presentation of 24 well insert (Reprocell europe), were pre-treated by soaking in 70% ethanol for 5 minutes with a subsequent wash in PBS for 5 minutes and a last wash in PBS for 1 minute. The inserts were transferred to a 12 well cell culture plate (Greiner bio-one).

Two different 3D models were created in this project. Caco-2 cells cultured with two different fibroblast cell lines separately: HDFn and CCD-18co. A schematic protocol of the culture is presented in the figure 6.

Caco-2 cells in co-culture with HDFn cells

220,000 HDFn cells from passage 6 to 7, were seeded in each pre-treated Alvetex® scaffold in a dropwise manner in 100 µL ensuring even coverage. Models were placed in a 37°C incubator (5% CO_2, 95% relative humidity) for two hours. When cells were attached to the scaffold, it was carefully

added 4.5 mL of complete DMEM media supplemented with 5ng/mL TGFβ1 (Life Technology) and 100µg/mL Ascorbic acid (Sigma-Aldrich). Media was changed every 3-4 days. At the 14th day of culture, 2 mL of complete DMEM media was added to the outer compartment and 220,000 Caco-2 cells from passage 52 to 54 were seeded covering the surface of the scaffold by dropping them in 100 µL. Cells were allowed to attach for 2 h and then it was top up media to 4.5 mL. The plate was placed to the incubator and media was changed every 2 days until differentiation at the 21st day of Caco-2 cells in culture.

Caco-2 cells in co-culture with CCD-18co cells

2 mL of complete DMEM media was added to the outer compartment of pre-treated Alvetex® inserts. 220,000 CCD-18co cells from PDL 25 to 41 or passage 4 to 11, were seeded in each scaffold in a dropwise manner in 100 µL ensuring even coverage. Models were placed in a 37°C incubator (5% CO_2, 95% relative humidity) for at least two hours. When cells were attached to the scaffold, it was carefully top up to 4.5 mL of complete MEM media. Media was changed every 2 days. At the 7th, 9th and 11th days of culture, 220,000 CCD-18co cells from PDL 25 to 41 or passage 4 to 11 were seeded in each insert. At the 14th day of culture, 2 mL of complete DMEM media was added to the outer compartment and 220,000 Caco-2 cells from passage 52 to 53 were seeded covering the surface of the scaffold by dropping them in 100 µL. Cells were allowed to attach for 2 h and then it was top up to 4.5 mL of complete DMEM media. The plate was placed to the incubator and media was changed every 2 days until differentiation at the 21st day of Caco-2 cells in culture.

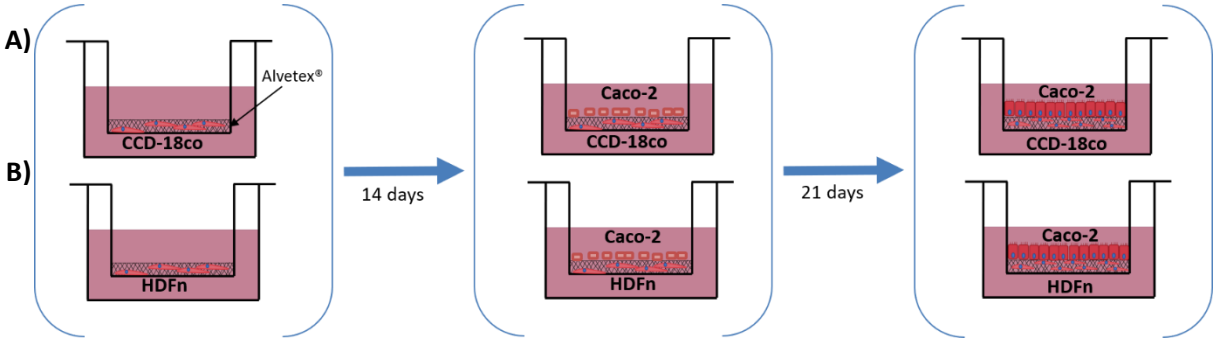

Figure 6: Schematic protocol of 3D models culture. A) 3D CCD-18co: Caco-2 cells in co-culture with CCD-18co cells in Alvetex® scaffold; and B) 3D HDFn: Caco-2 cells in co-culture with HDFn cells in Alvetex® scaffold.

2.3. Human tissue

Normal human duodenum small intestine sample was provided by Biopta Ltd in compliance with Human Tissue Act (HTA) regulations and the necessary consent.

2.4. Histology

2.4.1. Paraffin embedding

Culture media was removed from Alvetex® and Transwell® inserts and then they washed three times in PBS. Membranes were detached from their support to be transferred to a 12 well plate using forceps. Samples were fixed in 4% Paraformaldehyde at 4°C overnight. The next day, samples were washed twice in PBS for approximately 1 minute and then dehydrated in 30%, 50%, 70% and 90% ethanol for 15 min each at room temperature. Membranes were left in 95% ethanol overnight at 4°C. The next day, they were left in 100% ethanol for 30 min. Then, inserts were sectioned in half using a razor blade and then they were transferred to cassettes that were subsequently submerged in a beaker with Histoclear II (National Diagnostics) for 30 min. Melted paraffin wax (ThermoFisher) was add to the histoclear to make a total of 1:1 wax and histoclear, and the beaker was incubated at 64°C in an oven for a further 30 min. Then, the histoclear:wax solution was removed and replaced with melted wax, leaving the beaker incubating at 64°C for 30 min. The last step was repeated once.

Samples were removed from the cassettes and transferred into dispomoulds to be embedded in wax blocks. They were left to set at room temperature overnight. Sections of 7 µm of thickness were cut using a Leica RM2125RT microtome and they were mounted onto Superfrost plus microscope slides (ThermoFisher).

2.4.2. Optical Cutting Temperature compound (OCT) embedding

Culture media was removed from the Alvetex® and Tranwell® inserts and washed twice in PBS for approximately 1 minute each, then they were fixed in 1:1 methanol and acetone at -20°C for 10 minutes. Membranes were detached from their support and cut in half using a razor blade and they were then placed into a dispomould filled with OCT embedding medium (ThermoFisher) for one hour. Another dispomould was filled with OCT and inserts were then, transferred and orientated into it using forceps. The blocks were left to set for approximately 10 minutes on a metal support in a polystyrene cool box containing liquid nitrogen. After that, the blocks were stored in a -80°C freezer. Sections were cut at 6 µm using a cryostat and mounted onto Superfrost plus microscope

slides (ThermoFisher). They were left to dry for at least 30 minutes at room temperature and then they were immediately used in further procedures.

2.4.3. Epoxy resin embedding

Culture media was removed from the Alvetex® and Transwell® inserts and it was immediately fixed at room temperature for at least one hour into Karnovsky fixative: 2% paraformaldehyde, 2.5% glutaraldehyde and 0.1M Cacodylate Buffer pH 7.4 in deionised water. For the human tissue, it was dissected in pieces of 2x5x1 mm in a petri dish containing PBS using forceps and a scalpel, then they were fixed with Karnovsky fixative at 4°C overnight. Inserts and tissue were washed for three periods of 5 minutes each in 0.1M Cacodylate Buffer pH 7.6. They were then, fixed in a 1:1 ratio of 2% osmium tetroxide and 0.2M Cacodylate Buffer pH 7.4 for 1 hour at room temperature. Samples were washed for three periods of 5 minutes each in 0.1M Cacodylate Buffer pH 7.6 and the plate was wrapped with parafilm and stored at 4°C to continue the process next day.

Samples were gradually dehydrated in 50%, 70%, 90% ethanol in three periods of 5 minutes each and then in 100% ethanol in three periods of 10 minutes each. The membranes where detached from their supports and transferred into glass vials to be infiltrated with 1:1 solution of absolute ethanol and propylene oxide for 15 minutes on a rotator. Samples were then infiltrated with propylene oxide and 1:1 ratio of propylene oxide and epon resin (Agar Scientific) for 15 minutes each. Subsequently, they were infiltrated three times in epon for 1 hour each. Samples were cut in small sections so that they can fit into the moulds, using a razor blade. Finally, they were transferred and orientated into the moulds filled with epon resin, using a cocktail stick, and they were polymerised in a 64°C oven for at least 24 hours.

2.4.3.1. Toluidine blue staining

Semithin sections of 0.5 µm were cut using a glass knife with a Leica Ultracut S ultramicrotome and they were mounted onto Superfrost plus microscope slides (ThermoFisher), leaving them to dry on a hot plate. After that, two to three drops of toluidine blue were used to cover and dye the samples, placing the slides on the hot plate for 2 minutes. Then, slides were washed with deionised water and mounted with DPX (Agar Scientific) using glass coverslips. Images were obtained using a Leica ICC50HD microscope.

2.4.3.2. Transmission Electron Microscopy

Ultrathin sections of 70 nm for intestine models and 60 nm for human intestine tissue were cut using a Diatome ultra diamond knife with a Leica EM UC6 ultramicrotome and samples were collected onto a Copper 150 mesh grid. To stain the samples, each grid was placed onto a 1% uranyl acetate (alcoholic) drop in a petri dish using forceps for 10 minutes. The grids were then, rinsed up and down in two successive changes of deionised water for 15 seconds each using forceps. Samples were post stained, placing each grid onto a drop of lead citrate and avoiding CO_2 contamination by covering the petri dish. Then, they were rinsed up and down in two successive changes of deionised water for 15 seconds each. Samples were let dry at room temperature for at least 20 minutes. Stained samples were examined in a Hitachi H7600 transmission electron microscope using an accelerating voltage of 100 kV. Images were taken using an Advanced Microscopy Techniques (AMT) imaging system.

2.5. Immunocytochemistry

Slides with samples mounted from OCT blocks were submerged in deionised water for 5 minutes and then, they were transferred into a stain tray. Samples were incubated in blocking solution for 1 hour at room temperature. Blocking solution was made up of 20% dilution of neonatal calf serum in a solution of 0.4% Triton X-100 (Sigma-Aldrich) in PBS. Then, samples were incubated with their appropriate dilution of primary antibody in blocking solution (Table 1) at 4°C overnight.

Slides were washed three times in PBS for 10 minutes each, using a rocker. Samples were incubated with their appropriate dilution of secondary antibody in blocking solution for one hour at room temperature, covering from the light. Then, they were washed three times in PBS for 10 minutes each and mounted in Vectashield® hard-set antifade mounting medium with DAPI (Vector Laboratories) using a glass coverslip (ThermoFisher). Slides were left to dry for at least 20 minutes at room temperature using a slide book, then they were kept at 4°C until ready to be imaged. High-resolution images were obtained using a Zeiss 880 CLSM with airy scan and using objective Plan-Apochromat 63x/1.4 Oil DIC M27.

Table 1. Primary and secondary antibodies used for Immunocytochemistry.

Antibody	Code	Manufacturer	Species and Isotype	Dilution	Sample fixation
Anti-Occludin	SC-133256	Santa Cruz Biotechnology	Mouse monoclonal, IgG_{2b}	1:100	1:1 methanol/acetone
Anti-ZO-1	40-2200	Invitrogen	Rabbit polyclonal, IgG	1:100	1:1 methanol/acetone
Anti-Claudin 1	ab15098	Abcam	Rabbit polyclonal, IgG	1:200	1:1 methanol/acetone
Anti- E-Catherin	610182	BD Transduction Laboratories	Mouse, $IgG_{2a,\kappa}$	1:100	1:1 methanol/acetone
Anti-Mouse (Alexa Fluor® 594)	A21203	ThermoFisher	Donkey polyclonal, IgG (H + L)	1:1000	
Anti-Rabbit (Alexa Fluor® 488)	A21206	ThermoFisher	Donkey polyclonal, IgG (H + L)	1:1000	

2.6. Western Blot

Preparation of lysates for 2D models

Culture media was removed from Transwell® inserts and they were rinsed with cold PBS two times. Membranes were detached from their support by cutting Transwell® membranes with a razor blade. They were transferred into a centrifuge tube with 150 µL of 1:100 protease and phosphatase inhibitor cocktail (ThermoFisher) in MPER buffer (ThermoFisher) using forceps. Membranes were broken using a tip and kept on ice for 30 minutes, vortexing every 5 minutes for periods of 10 seconds each. Samples were stored at -20°C until required.

Preparation of lysates for 3D models

Culture media was removed from Alvetex® inserts and they were rinsed with cold PBS two times. Membranes were unclipped from their support and transferred into a 12 well plate. 75 µL of 1:100 protease and phosphatase inhibitor cocktail (ThermoFisher) in MPER buffer (ThermoFisher) was added to the surface of the insert and, using a tip, it was scratched trying to dislodge only epithelial cells. Lysates where then collected into a named centrifuge tube. Another 75 µL of 1:100 MPER solution were added to the surface of the insert to collect as much as possible of epithelial cells proteins. Samples were kept on ice for 30 minutes, vortexing every 5 minutes for periods of 10 seconds each and were stored at -20°C until required.

Sample and gel preparation

It was measured the protein concentration of each sample using a Bradford assay. To prepare a standard curve, it was used proteins standards of 2, 1.5, 1, 0.7, 0.5, 0.25 and 0.125 mg/mL (Bio-Rad). Following instructions from the manufacturer, samples were left to incubate with the dye reagent (Bio-Rad) for 10 minutes at room temperature. MPER buffer was used as a blank. Then, it was read the absorbance of each sample in a plate reader at 595 nm.

It was calculated the concentration of protein in each sample and 10 µg of protein was diluted in a proportion 1:4 with 10% 2-mercaptoethanol (Sigma-Aldrich) in 4X Laemmli buffer (Bio-Rad). Then, samples were boiled at 95°C for 10 minutes in a heat block.

SDS-PAGE gels were made using the following recipes in table 2. It was also used a 4-20% precast protein gel (Bio-Rad).

Table 2. Components required to make two 1.5 mm SDS_PAGE gels for Western blot.

Components	5% Stacking Gel	10% Resolving gel
Deionised water	5.625 mL	10.6 mL
Prosieve acrylamide	750 µL	4 mL
1.5M Tris pH 6.8	1 mL	-
1.5M Tris pH 8.8	-	5 mL
10% SDS	75 µL	200 µL
10% APS	75 µL	200 µL
Temed	7.5 µL	10 µL

Electrophoresis and electrotransfer

It was loaded a total of 10 µg of protein on the gels and they were run at 100 V.

Proteins were electrotransferred to a 0.45 µm pore size nitrocellulose membrane (GE Healthcare Life Sciences) at 250 mA at room temperature for 2 h for the 10% gel; and at 25 V at 4°C overnight and then 50 V at 4°C for 2 h for the 4-20% precast protein gel (Bio-Rad).

Blocking, incubation and detection

Membranes were blocked in blocking buffer (1X TBST with 5% skimmed dry milk) for 2 h using a rocker. Then, they were incubated with the primary antibodies listed in the table 3 with their respective dilution in blocking buffer at 4°C overnight. Membranes were washed with 1X TBST three times for 10 minutes each and then they were incubated with their respective secondary antibody for 1 h at room temperature. They were washed with TBST three times for 5 minutes each and developed with Clarity Western ECL system (Bio-Rad) for 2 minutes.

Table 3. Antibodies used for Western blot.

Antibody	Code	Manufacturer	Species and Isotype	Dilution
Anti-Occludin	SC-133256	Santa Cruz Biotechnology	Mouse monoclonal, IgG_{2b}	1:1000
Anti-ZO-1	40-2200	Invitrogen	Rabbit polyclonal, IgG	1:1000
Anti-Claudin 1	ab15098	Abcam	Rabbit polyclonal, IgG	1:1000
Anti-E-Catherin	610182	BD Transduction Laboratories	Mouse, $IgG_{2a,k}$	1:10,000
Anti-beta Actin	ab8224	Abcam	Mouse monoclonal, IgG_1	1:20,000
Anti-GAPDH	ab9485	Abcam	Rabbit polyclonal, IgG	1:10,000
Anti-Mouse HRP	A4416	Sigma-Aldrich	Goat polyclonal, IgG (H + L)	1:4000
Anti-Rabbit HRP	AP182P	Millipore	Donkey polyclonal, IgG	1:20,000

2.7. RT-qPCR

Preparation of lysates from 2D cultures

Cell culture in flasks

Culture media was aspirated from the flasks and then they were washed in cold PBS two times. 200 µL of buffer RLT (QUIAGEN) was placed in the surface where the cells are attached. Using a cell scratcher, cells were dislodged, and lysates were collected in a centrifuge tube to be immediately stored at -80°C until required.

2D models

Culture media was removed from the Transwell® inserts and then, they were washed two times in cold PBS. 200 µL of buffer RLT (QUIAGEN) was added in the surface of the membrane and it was scratched using a tip to dislodge cells, taking care not to brake the membrane. Lysates were collected in a centrifuge tube and they were stored at -80°C until required.

Preparation of lysates from 3D cultures

Culture media was removed from the Alvetex® inserts and then, they were washed two times in cold PBS. Inserts were unclipped from their support and then they were transferred to a 12 well plate. 200 µL of buffer RLT (QUIAGEN) was added in the surface of the membrane and it was scratched using a tip trying to dislodge only epithelial cells. Lysates were collected in a centrifuge tube and they were stored at -80°C until required.

RNA extraction

Lysates were homogenised five times using a 21 g needle (BD). 200 µL of ethanol was added to the samples mixing them up and then they were transferred into a RNeasy spin column (QUIAGEN) to centrifuge at 8,000 xg for 15 seconds. Then, it was added 700 µL of RW1 buffer (QUIAGEN) into the column, to subsequently centrifuge at 8,000 xg for 15 seconds. 30 µL of a DNase solution (Promega) containing 80% Yellow Core Buffer, 10% $MnCl_2$ 0.09 M and 10% DNase was added to each sample into the column and it was left incubating for 15 minutes at room temperature. Samples where then washed with 500 µL of RPE buffer (QUAGEN) and they were centrifuge at 8,000 xg for 15 seconds. Another wash with 500 µL of RPE buffer was done, centrifuging at 8,000 xg for 2 minutes this time. Finally, samples were collected in a RNase free centrifuge tube adding 25 µL of Nuclease free water and centrifuging at 8,000 xg for 1 minute. The quantity and quality of RNA obtained were assessed by using a NanoDrop 1000 Spectrophotometer. Samples with $A_{260/280}$ ratio of 1.8-2.1 were selected to continue with the reverse transcription.

Reverse transcription

To conduct the reverse transcription of the samples, it was used GoScript™ Reverse Transcription Mix, Oligo(dT) (Promega). Following the protocol provided for the kit, it was calculated the amount of sample to dilute 500 ng of RNA in nuclease free water, making a total of 14 µL per sample. 4 µL of reaction buffer, Oligo(dT), 2 µL of enzyme mix and 14 µL of experimental RNA were mixed in a

tube. Tubes were briefly centrifuge and then placed in a thermocycler. Samples were incubated using the following protocol:

Temperature	Time	Number of cycles
25°C	5 min	1
42°C	60 min	1
70°C	15 min	1
4°C	∞	

The cDNA samples were stored at -20°C until required.

Real-time PCR

It was used BioRad SsoAdvanced Universal SYBR® Green Supermix to carry on the qPCR. cDNA samples were diluted with nuclease free water to obtain a concentration of 5 ng/µL. To make 10 µL of reaction per sample, it was prepared enough amount of the following master mix for all the samples:

Component	Volume needed per 10 µL reaction
SsoAdvanced universal SYBR green supermix (2x)	5 µL
Primers mix (1:1 100 µM Forward and Reverse primers, see table 4)	0.5 µL
Nuclease free H_2O	1.5 µL

Master mix was carefully mixed to ensure homogeneity and equal amount was added into each well of a 96-well PCR plate (BioRad). Then, 3 µL of cDNA template was added into each well. PCR plate was sealed and centrifugated at 8,000 x*g* for 2 minutes to ensure all liquid was at the bottom of the wells. PCR plate was then placed in a CFX Connect Real-Time PCR Detection System (BioRad) and the following protocol was run:

Cycling condition	Temperature	Time
Initial denaturation	95°C	30 sec
X40 cycles:		
Step 1	95°C	5 sec
Step 2	60°C	15 sec

Table 4. Primers used for real-time PCR to assess junctional complexes gene changes in expression in intestinal tissue models. Oligos sequences were taken from Yamaguchi *et al*., 2010 and Zhu *et al*., 2017 and produced by Sigma.

Gene	Primer sequence (5'-3')	
	Forward	**Reverse**
GAPDH*	ACCACAGTCCATGCCATCAC	TCCACCACCCTGTTGCTGTA
Villin*	AGGATGATGTGTTCCTACTAGATGTCTG	GTTGCTGCGGCCTTCTTC
Occludin*	CTCCCATCCGAGTTTCAGGT	GGAGTGTAGGTGTGGTGTGT
ZO-1	CGGTCCTCTGAGCCTGTAAG	GGATCTACATGCGACGACAA
Claudin-1	AACGCGGGGCTGCAGCTGTTG	GGATAGGGCCTTGGTGTTGGGT
E-Cadherin*	CTGAGAACGAGGCTAACG	TTCACATCCAGCACATCC

*Linear efficiency of each set of primers was previously of this work evaluated by series of 3 template concentrations.

2.8. Transepithelial Electrical Resistance

It was used a Millicell® ERS-2 Electrical Resistance System. Before starting to measure, electrode was disinfected with 70% ethanol and then washed with PBS. Following the protocol described in figure 7, the electrodes were immersed and held steady at 90° angle so that the shorter tip was in the insert, taking care not to contact cells growing on the membrane, and the longer tip was in the outer well. For the blank, it was measured the electrical resistance of an insert with the correspondent culture media without cells growing on it.

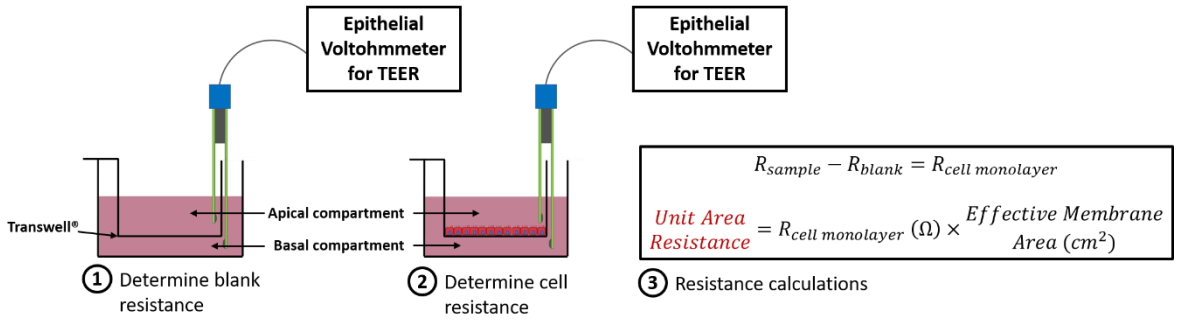

Figure 7: Schematic protocol of TEER measurement in the intestinal models. 1) Electrodes were immersed into the wells so that the shorter tip is in the apical compartment and the longer tip is in the basal compartment. Electrodes were held at a 90° angle to the bottom of the well. To obtain the blank, it was measured a cell culture insert with the relevant media and without cells. 2) The same procedures were followed to determine cell resistance in each model. 3) Calculations were made to obtain the unit area resistance.

2.9. Statistical analysis

All reported values were expressed as mean ± standard error of the mean (SEM) and they were analysed using the software GraphPad Prism 5.0. Further explanation about statistical analysis are provided in the result section for each experiment.

3. Results

3.1. Human small intestine

Normal human small intestine tissue was provided fixed in Karnovsky solution and then it was embedded in epoxy resin. 0.5 µm thick sections were stained with toluidine blue in order to observe the structure of the small intestine mucosa. In the figure 8a it could be appreciated the layers of the intestine mucosa comprising the lamina propria and epithelium as indicated.

Subsequently, 60 nm sections were visualised in the Transmission Electron Microscopy in order to evaluate structures that were not easy to observe at low magnification. In the figure 8b can be observed the presence of microvilli at the surface of the epithelium at low and high magnification.

A)

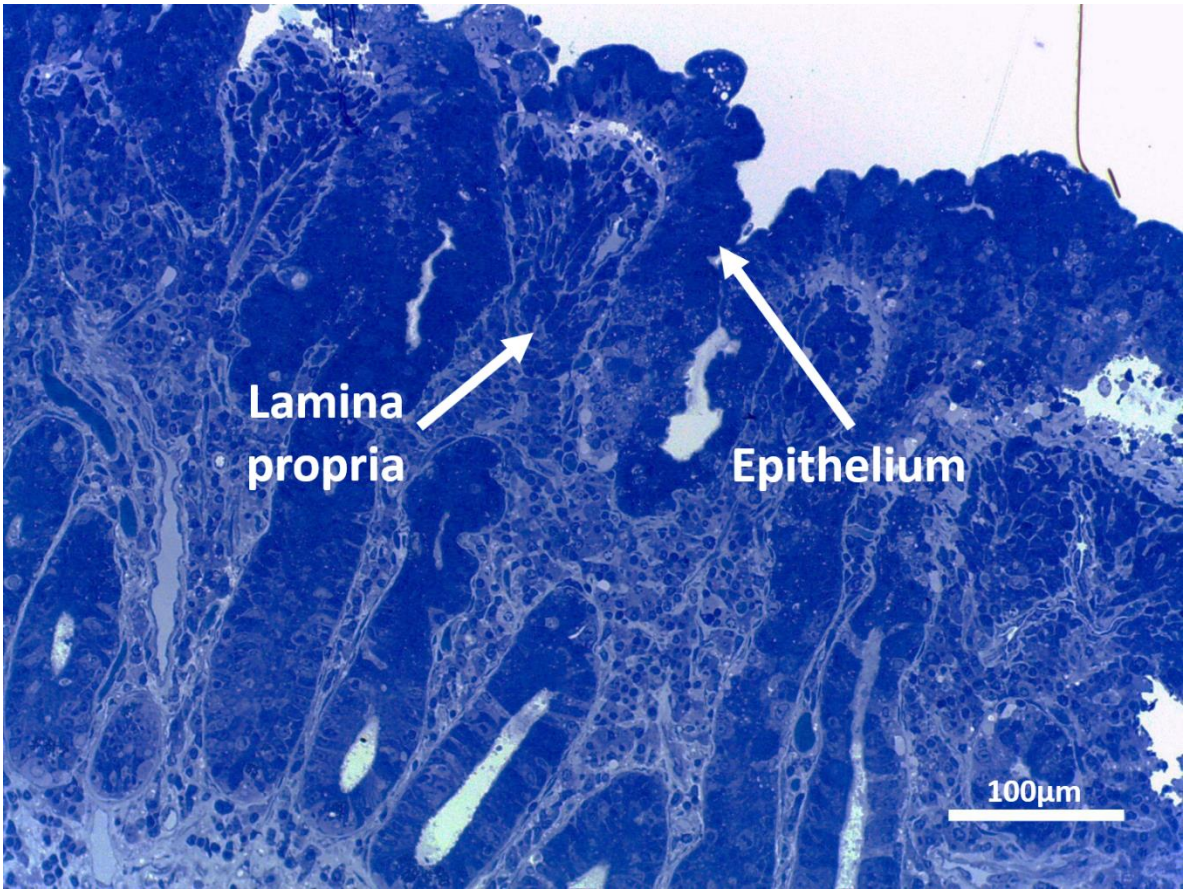

B)

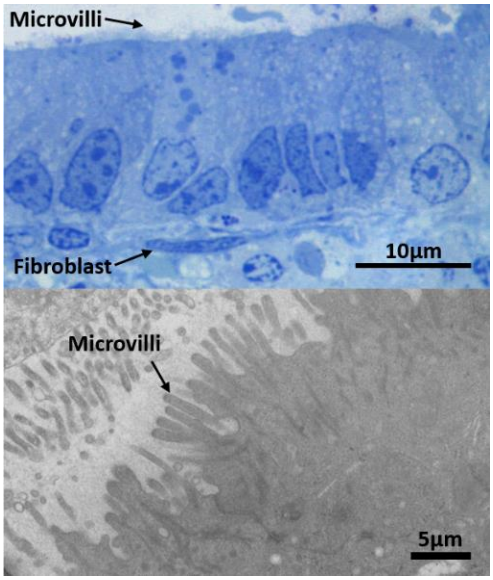

Figure 8: Human small intestine histology. A) Toluidine blue 0.5 µm thick section of small intestine mucosa. B) Toluidine blue 0.5 µm thick section of small intestine epithelium and brush border electron micrograph.

Electron micrographs of the epithelial cell apical lateral membranes revealed the presence of junctional complexes. In the figure 9 it was identified the development of tight junctions, adherens junctions and desmosomes.

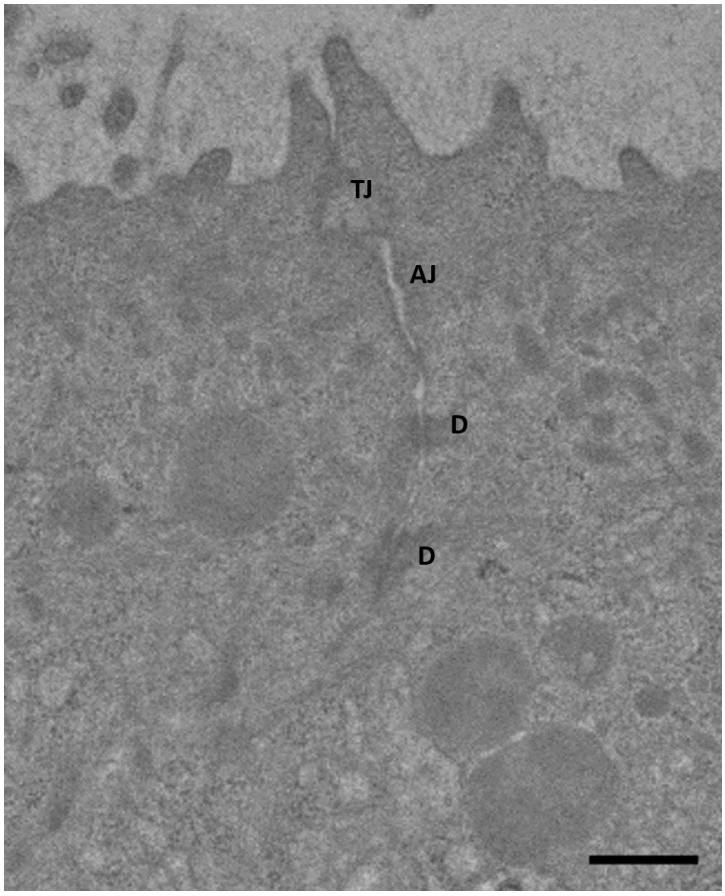

Figure 9: Schematic representation of junctional complexes localization in the small intestine epithelial cells. Electron micrograph of an apical region of human small intestine epithelium. Tight junctions are signalled as TJ, adherens junctions as AJ, and desmosomes as D; scale bar: 0.5 µm.

3.2. 2D Culture Models

3.2.1. Construction of 2D models and Caco-2 cells morphology

Caco-2 cells were cultured in Transwell® inserts and maintained with conditioned media until differentiation for 21 days. In parallel, untreated Caco-2 cells were cultured in Transwell® inserts to be used as the control. Caco-2 cells acquired morphologic characteristics of enterocytes including the development of microvilli and the polarization of the cells after 21 days of culture (figure 10).

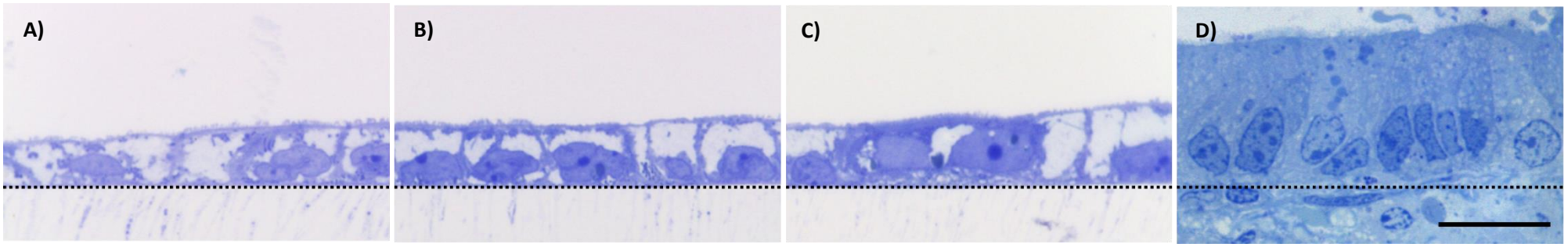

Figure 10: Morphology of 2D models. Toluidine blue 0.5 µm sections of A) 2D CCD-18co: Caco-2 cells cultured in Transwell® inserts and maintained with CCD-18co cells conditioned media until differentiation; B) 2D HDFn: Caco-2 cells cultured in Transwell® inserts and maintained with HDFn cells conditioned media until differentiation; C) Control: Caco-2 cells cultured in Transwell® inserts and maintained with DMEM; and D) Small intestine human tissue. With exception of human tissue, it was taken images from at least 3 independent samples for each model; for human tissue it was taken images from a single sample. Basement of epithelial cells is delimited with a non-continuous line. Scale bar: 10 µm.

Electron micrographs were taken to detailed observe the development of junctional complexes in the Caco-2 lateral plasma membranes (LPM) (figure 11). In those micrographs, JC are observed as dense features along the LPM. Also, it was observed in a higher magnification, the presence of microvilli in all the models and in the native intestinal tissue.

From morphological analysis it was observed that when Caco-2 cells are cultured in Transwell® they had a shorten height, resembling a cuboidal shape which is in contrast with the columnar epithelial structure observed in real human intestinal tissue.

To compare those observations between the models and native tissue, morphometrics analysis were carried out. Electron micrographs were taken from each tissue and the heights and widths of single epithelial cells were measured using ImageJ software (figure 12). The ratio between the height and width of a single epithelial cell was calculated, meaning that below the unit, cells are more flattened, and above the unit, cells are more elongated.

The data indicate that the paracrine effect influences the elongation and shape of Caco-2 cells while non-treated control models presented a more flattened cuboidal structure. Native tissue presented a classic simple columnar epithelium, as expected.

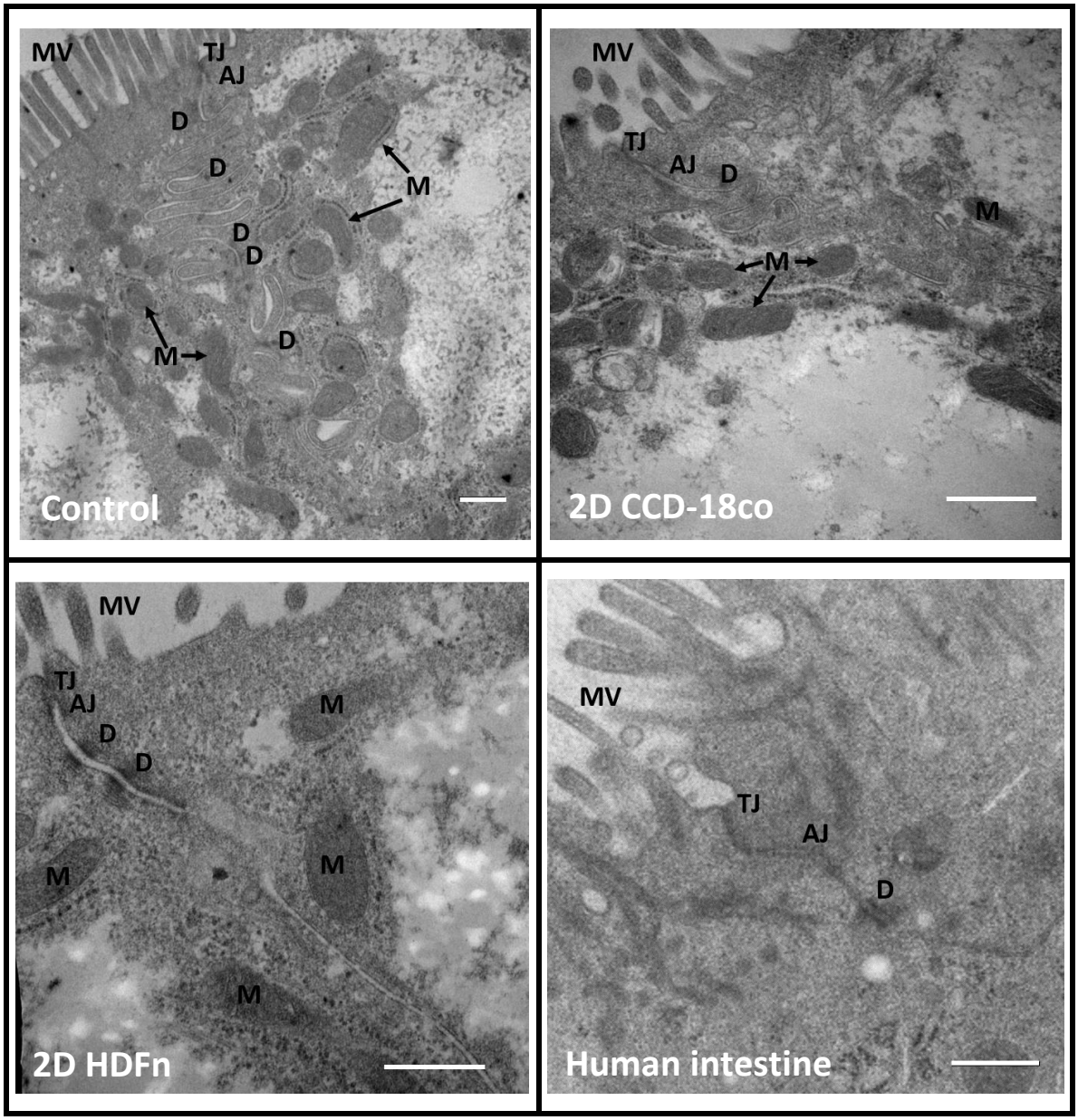

Figure 11: Ultrastructural features of Caco-2 cells in 2D models and human small intestine epithelial cells. At 21 days of culture, functional differentiation of Caco-2 cells are defined by the appearance of junctional complexes and development of microvilli. TJ= tight junctions, AJ= adherens junctions, D= desmosomes, MV microvilli, M= mitochondria. Scale bars= 0.5µm.

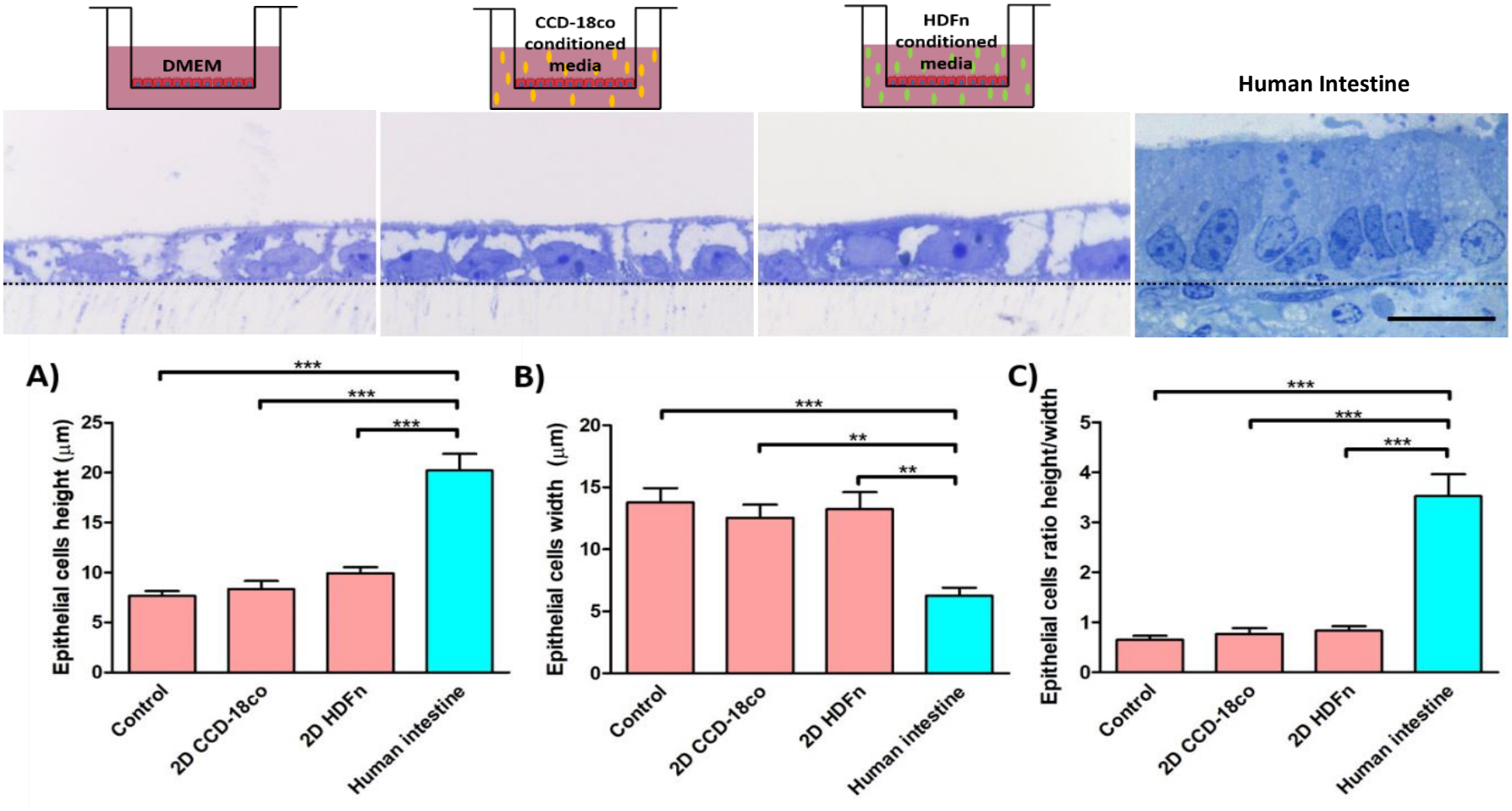

Figure 12: Morphometric analysis of epithelial cells in 2D models. A) Measurements of epithelial cells heights in 2D models; and human small intestine. B) Measurements of epithelial cells widths in 2D models; and human small intestine. C) Ratio between the height and width of epithelial cells in 2D models and human small intestine. With exception of human intestine, 5 cells were measured from 3 different independent samples giving a total of n=15; for human intestine n=10 from a single sample. Error bars represent the standard error of the mean (SEM). It was run a One-way ANOVA analysis and Tukey Multiple Comparison Test ($P < 0.05$). To state that figure of toluidine blue sections represented above graphs is the same as figure 10 and were included in figure 12 for comparison purposes. Analysis revealed that while Caco-2 cells in 2D models present a cuboidal morphology, human epithelium in the small intestine present a columnar morphology. Moreover, Caco-2 cells in paracrine effect models showed an increase of height and decrease of width, resembling human small intestine. Scale bar= 10µm.

Electron micrographs were taken of the full length of the LPM between Caco-2 cells to detect changes in their structure between the models and real tissue (figure 13). Remarkably, the paracrine effect of fibroblast cell lines on Caco-2 has been shown to reduce the LPM folding, similar to the human intestinal tissue with more straighten membranes. A reduction in the electron-dense junctional complexes along the LPM of Caco-2 cells in paracrine effect models was also detected which was consistent with what was observed in native tissue.

A)

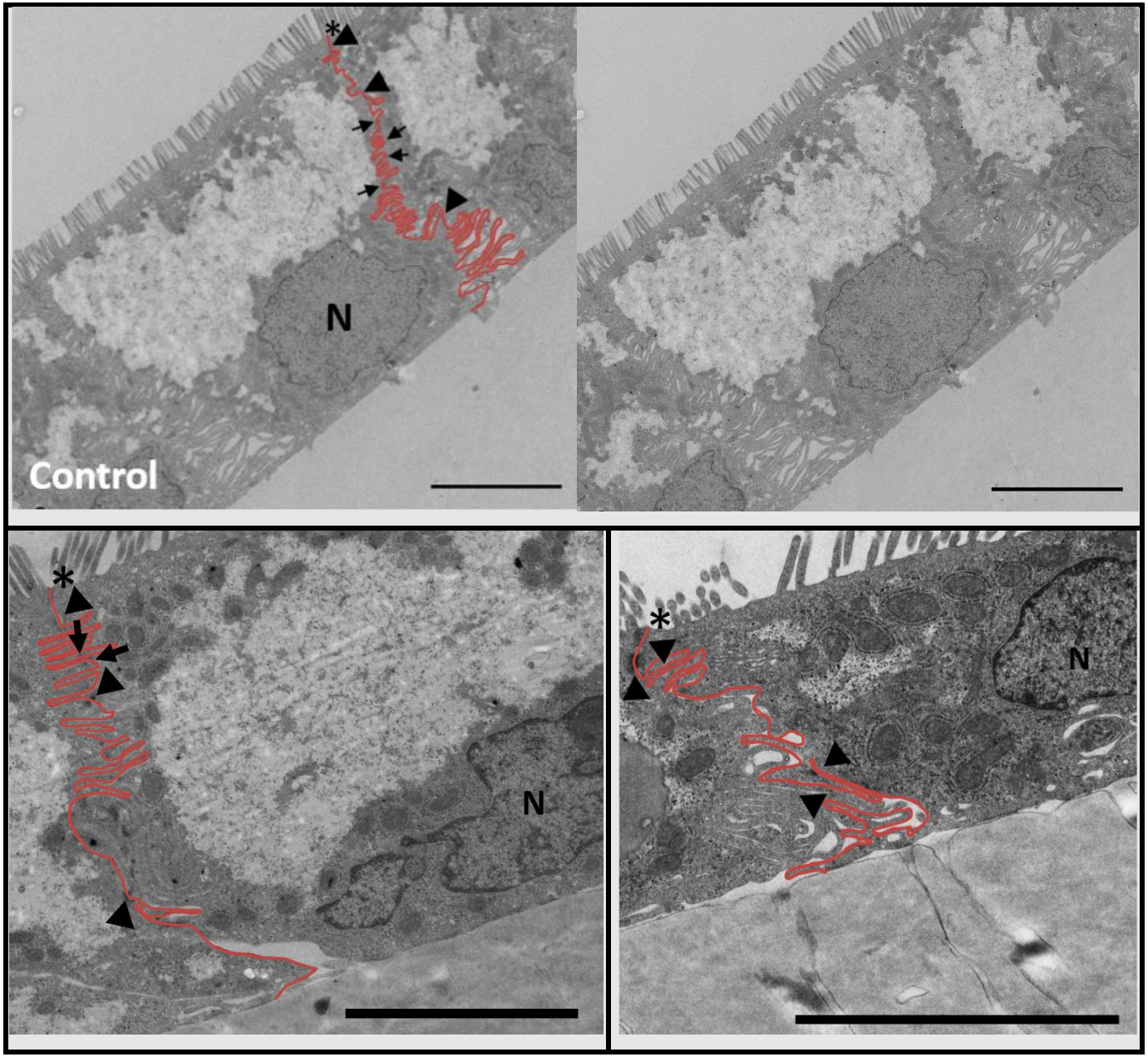

B)

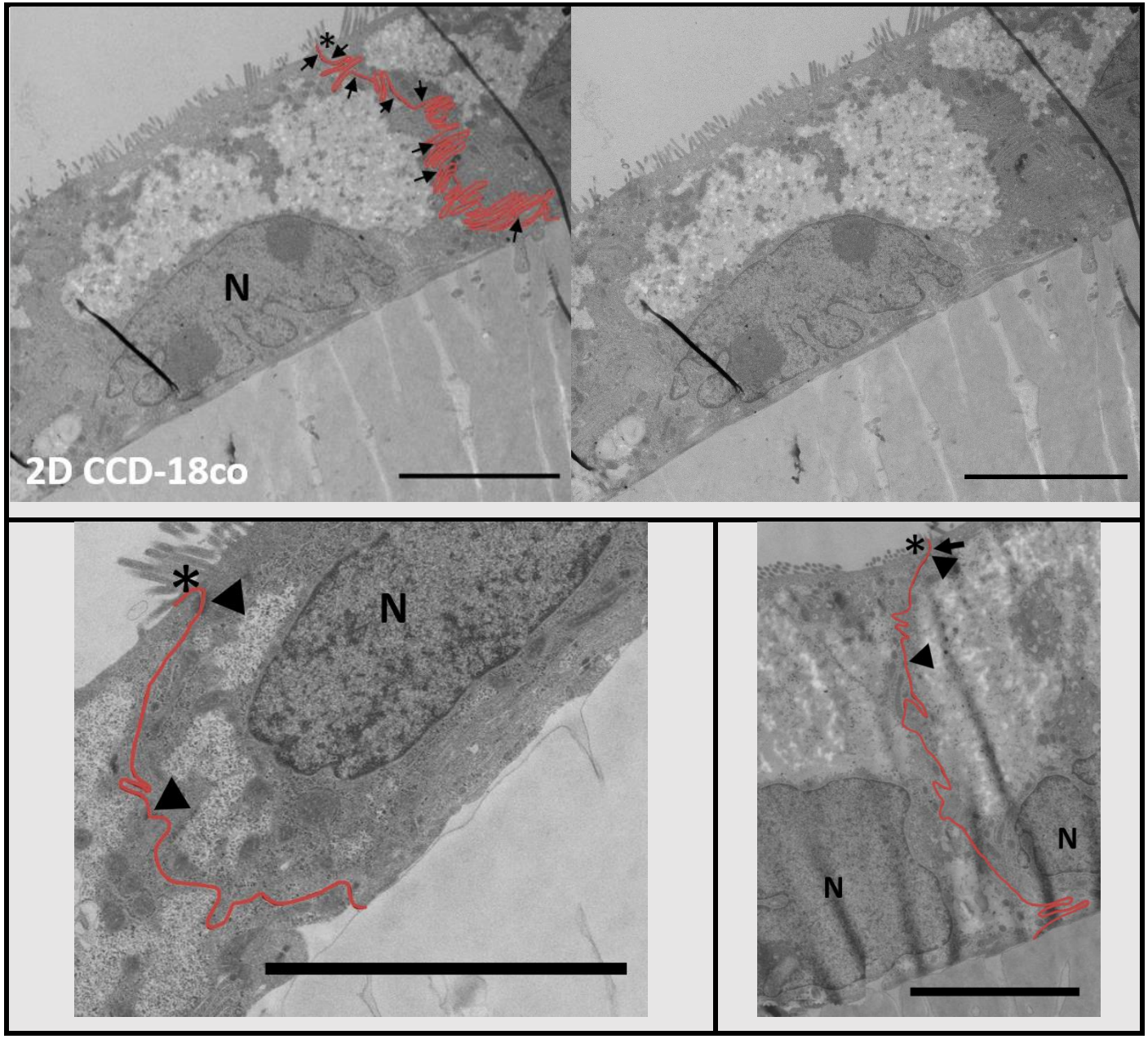

C)

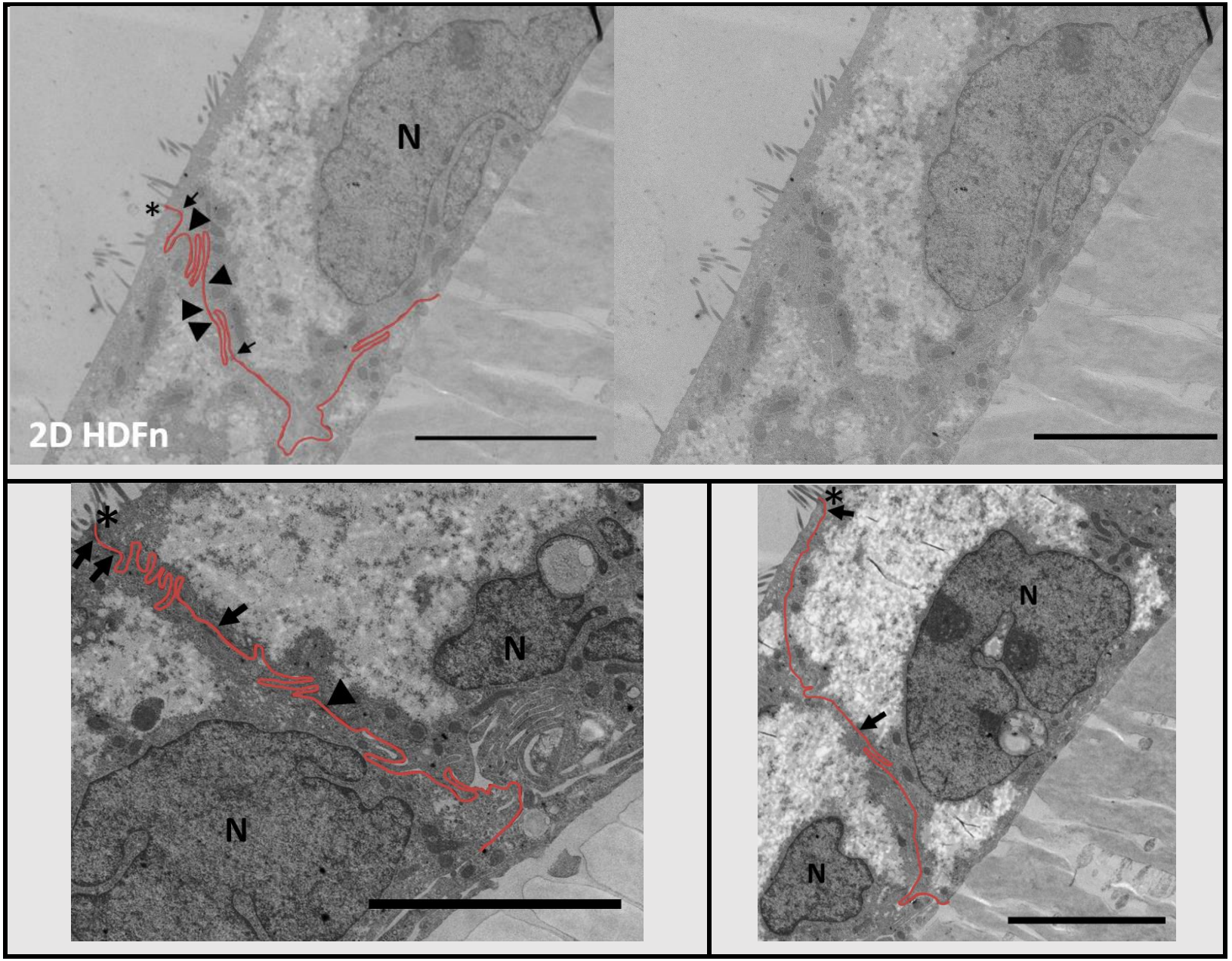

D)

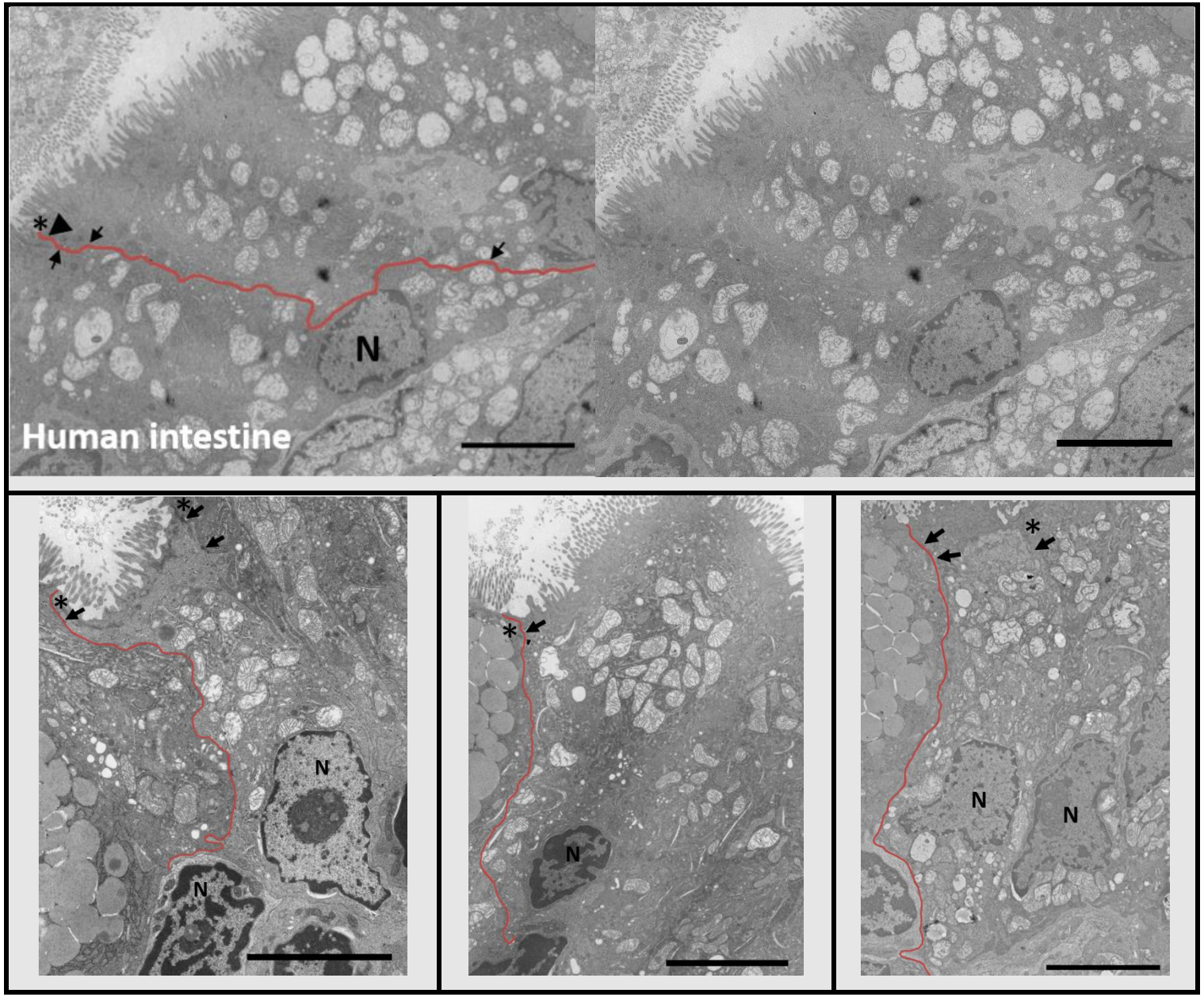

Figure 13: Electron micrographs of epithelial cells in 2D models. Electron micrograph of lateral membranes in caco-2 only culture as control model (A), CCD-18co paracrine model (B), HDFn paracrine model (C), and human small intestine (D). Epithelial lateral membranes are emphasised in salmon colour; tight junctions are indicated with asterisks; desmosomes with arrows; and adherent junctions with head arrows. N= nuclei, scale bars: 5 µm.

Further analysis was undertaken where the length of the lateral membranes was measured to determine whether there was a relationship between the LPM folding with cell height (figure 14 a, b). Results from figure 14a revealed that 2D HDFn paracrine model presented a significant reduction in the LPM length. It was also observed a reduction in the 2D CCD-18co model, even though it was not significant in comparison with the control. From figure 14b it was revealed that while paracrine effect models present greater epithelial cell heights, the decrease of the LPM folding is reflected with the decrease in the LPM length. It is important to notice that even when the control and 2D CCD-18co models increase the lateral membrane in comparison with native tissue, 2D HDFn model presented lower measurements than native tissue (figure 14a). This could be explained by the fact that although native tissue presents more straighten membranes, the epithelium is taller resulting in a naturally longer LPM.

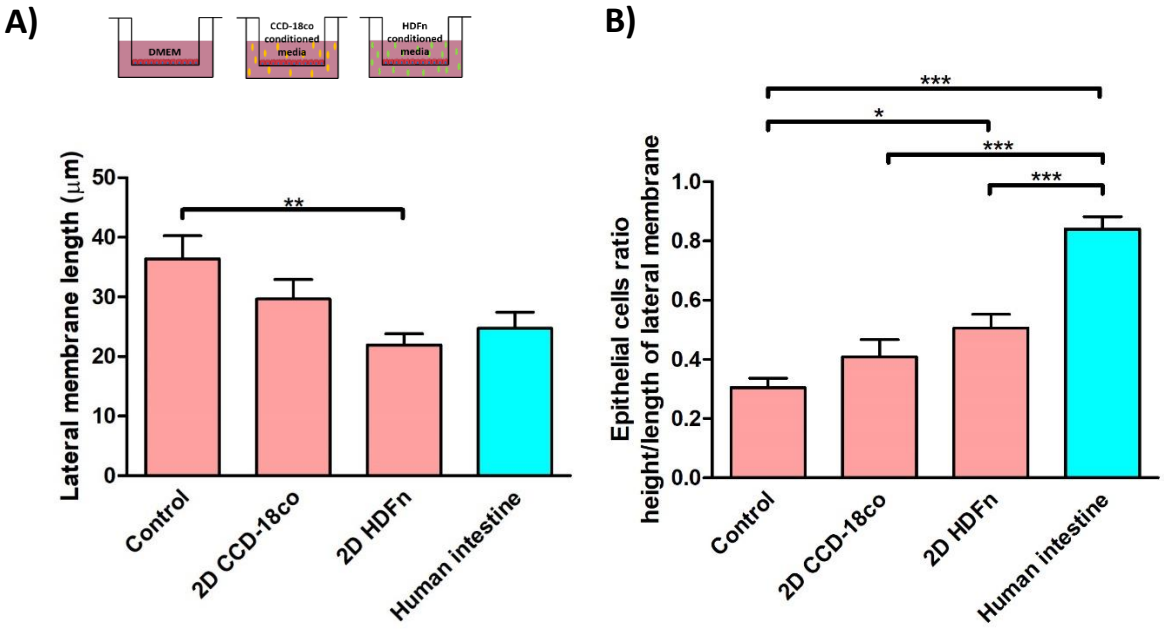

Figure 14: Morphometric analysis of epithelial cells lateral membranes in 2D models. A) Analysis of the epithelial lateral membrane lengths in 2D models for n=25 cells measured for at least 3 independent samples; and in human small intestine for n=10 cells measured for a single sample. B) Ratio between the height and lateral membrane length of epithelial cells in 2D models and human small intestine. Caco-2 only culture as the control model. Error bars represent the standard error of the mean (SEM). An analysis One-way ANOVA demonstrated a significant variation of lateral membrane length among conditions with P=0.0087 (A) and P=0.0001 (B). A post hoc Tukey Multiple Comparison Test revealed that HDFn paracrine model present a significant reduction at $P < 0.05$ in the lateral membrane length compared than control model.

3.2.2. Transepithelial Electrical Resistance Profiles

To assess the integrity of the Caco-2 barrier in 2D models, it was being measured the Transepithelial Electrical Resistance (TEER) every 6 days and in the last day of culture (figure 15). Following the instructions from the volthometer manual (figure 8), it was measured the electrical resistance of each model and inserts with no cells growing were measured as blank. Further calculations were made to obtain the unit area resistance expressed in $\Omega \cdot cm^2$. Paracrine effect models showed a decrease in the TEER values from the first day of measurement (day 6th of culture) compared than the untreated model. This finding suggests that paracrine effect models develop, to a lesser extent, tight junction proteins and it encouraged to study the expression of those proteins in molecular levels.

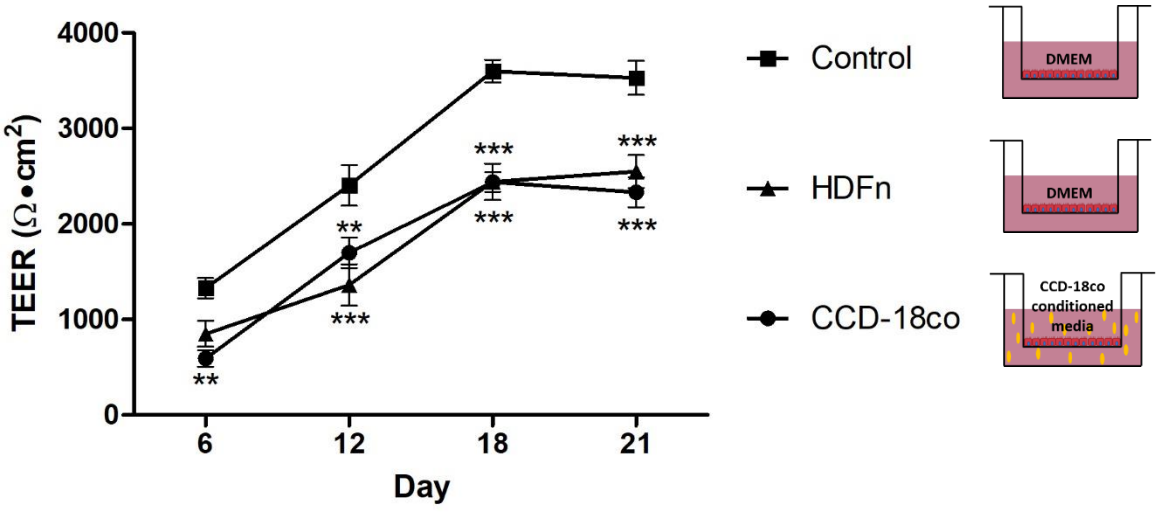

Figure 15: Transepithelial electrical resistance (TEER) profiles of Caco-2 cells 2D models. Error bars represent the standard error of the mean (SEM). Two-way ANOVA analysis and Bonferroni post test revealed that during the different days of culture, control model TEER values increased significantly in comparison with paracrine effect models (** P < 0.01, *** P < 0.001, n=17 independent samples).

3.2.3. mRNA expression of junctional complexes

Expression profiling qPCR analysis was conducted in order to study changes of junctional complexes gene expression in the paracrine models. mRNA was extracted at the end of culture for each model. For each qPCR run, it was analysed one biological repeat of each experimental group and the same control sample was loaded in all of them. For each gene of interest, each cDNA sample was loaded for triplicate and the average of the Ct values was calculated. It was used GAPDH as reference gene

to normalise those values. ΔCt was calculated by subtracting the averaged Ct values of GAPDH from the averaged Ct values of the gene of interest. Then, ΔΔCt for each gene was calculated by subtracting the ΔCt values of the control from the ΔCt values of the experimental group. Finally, it was calculated the mRNA relative expression using the equation $2^{-\Delta\Delta Ct}$. A total of 3 independent samples or replicas of each model and control were evaluated. Each model replica was normalized to their respective control replica. At the end, control variance was calculated by choosing one replica and expressing the others as a relative proportion. It was observed that occludin, claudin-1 and E-cadherin junctional complexes decreased in the paracrine effect models compared than non-treated model.

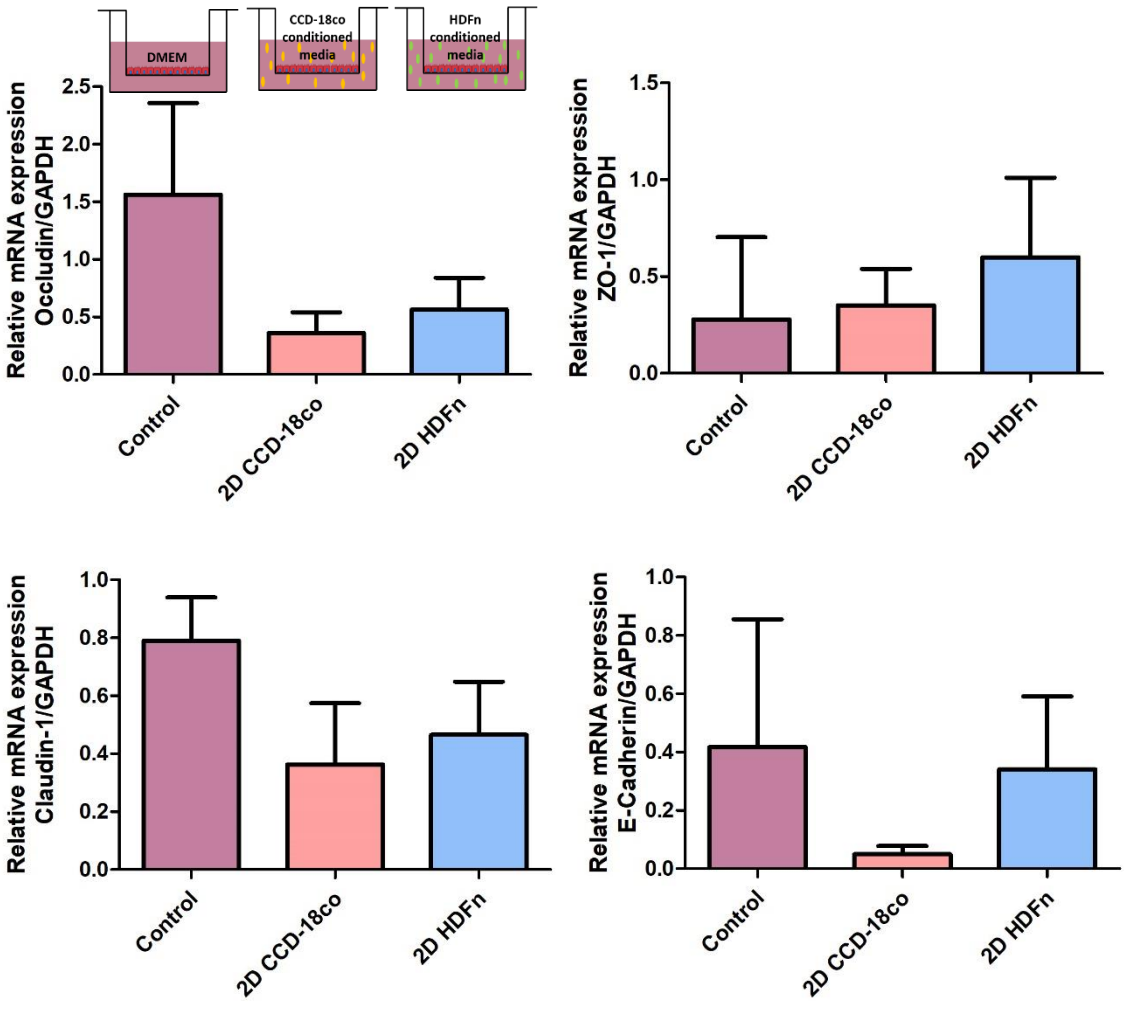

Figure 16: Analysis of the junctional proteins gene expression in 2D models. Variation in the gene expression of tight junction proteins (occludin, ZO-1 and claudin-1) and adherens junction (E-cadherin) in 2D models were analysed. Error bars represent the standard error of the mean (SEM), a total of n=3 independent samples.

Analysis demonstrated downregulation of occludin, claudin-1 and E-cadherin genes in paracrine effect models.

3.2.4. Protein expression of junctional complexes

To assess the expression of junctional proteins in 2D models, samples were analysed by Immunostaining. Samples of each kind of model were fixed in 1:1 methanol/acetone before being embedded in OCT compound. 7 µm sections of each model were immunostained against occludin, ZO-1, Claudin-1 and E-Cadherin junctional proteins in order to study changes in their expression between the different models (figure 17).

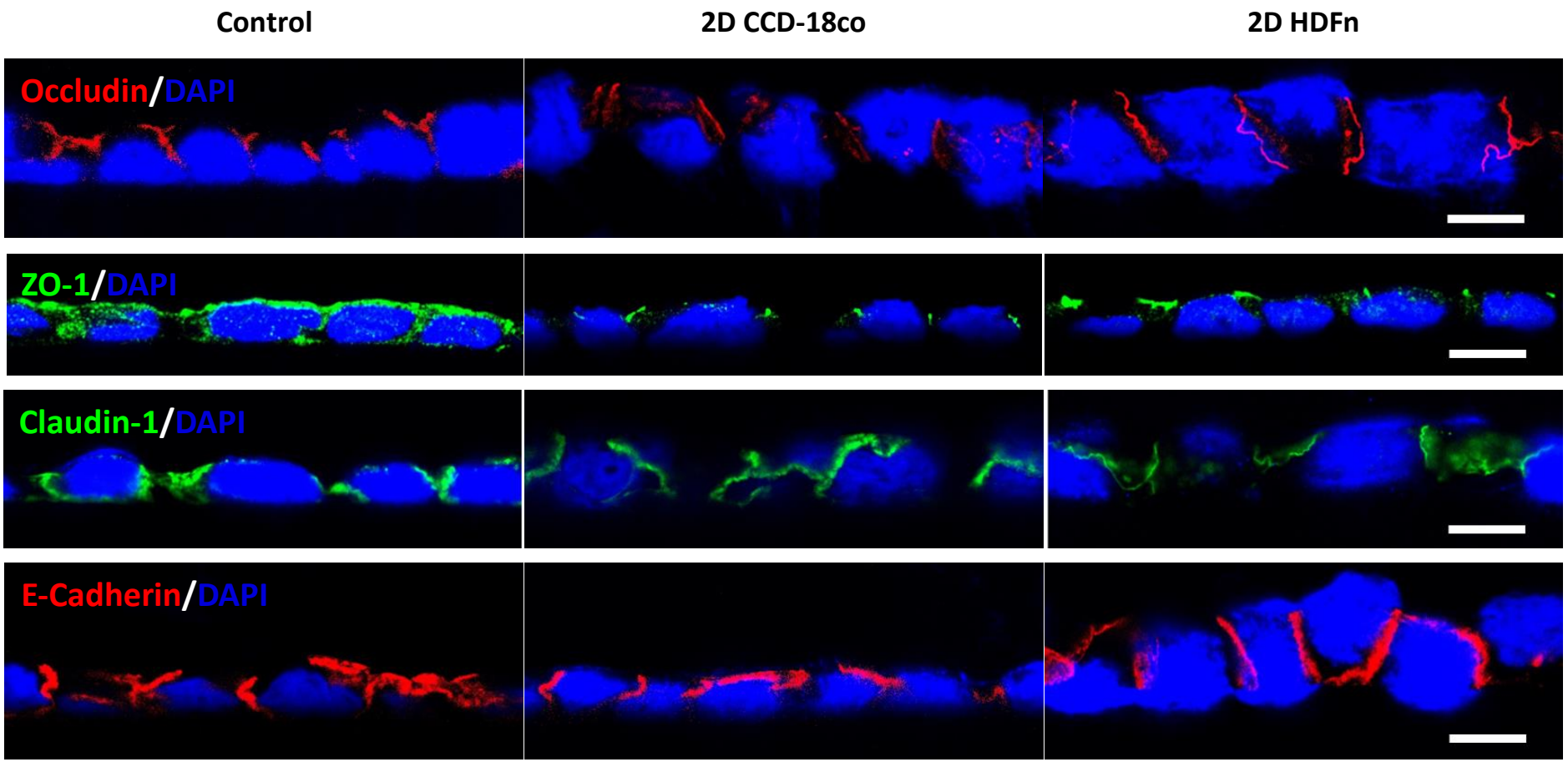

Figure 17: Immunofluorescence analysis of junctional proteins expression in 2D models. Paracrine effect intestinal models decrease the expression of Occludin, ZO-1, claudin-1 and E-cadherin proteins compared than conventional intestinal model. Confocal microscopy of Caco-2 cells monolayers cultivated on Transwell® inserts for 21 days and fed them with conditioned media from CCD-18co and HDFn fibroblasts, and with DMEM for the control model. OCT embedded sections fixed in 1:1 methanol/acetone were incubated with the primary antibody against junctional complexes, followed by the corresponding secondary antibody. Nuclei were counterstained with DAPI. Pictures were taken from a single sample for each model. Scale bars: 10 µm.

Immunostaining showed that each model expressed each of the different junctional complexes. A significant loss of these proteins was observed in the paracrine treated models. TEM pictures also revealed the location of junctional complexes and, as a way to compare their expression between the models and human tissue, the total number of electron-dense features observed along the lateral membranes was quantified (figure 18). Results revealed not statistically significant differences in the number of junctional complexes expressed along the LPM of each model and human intestine tissue.

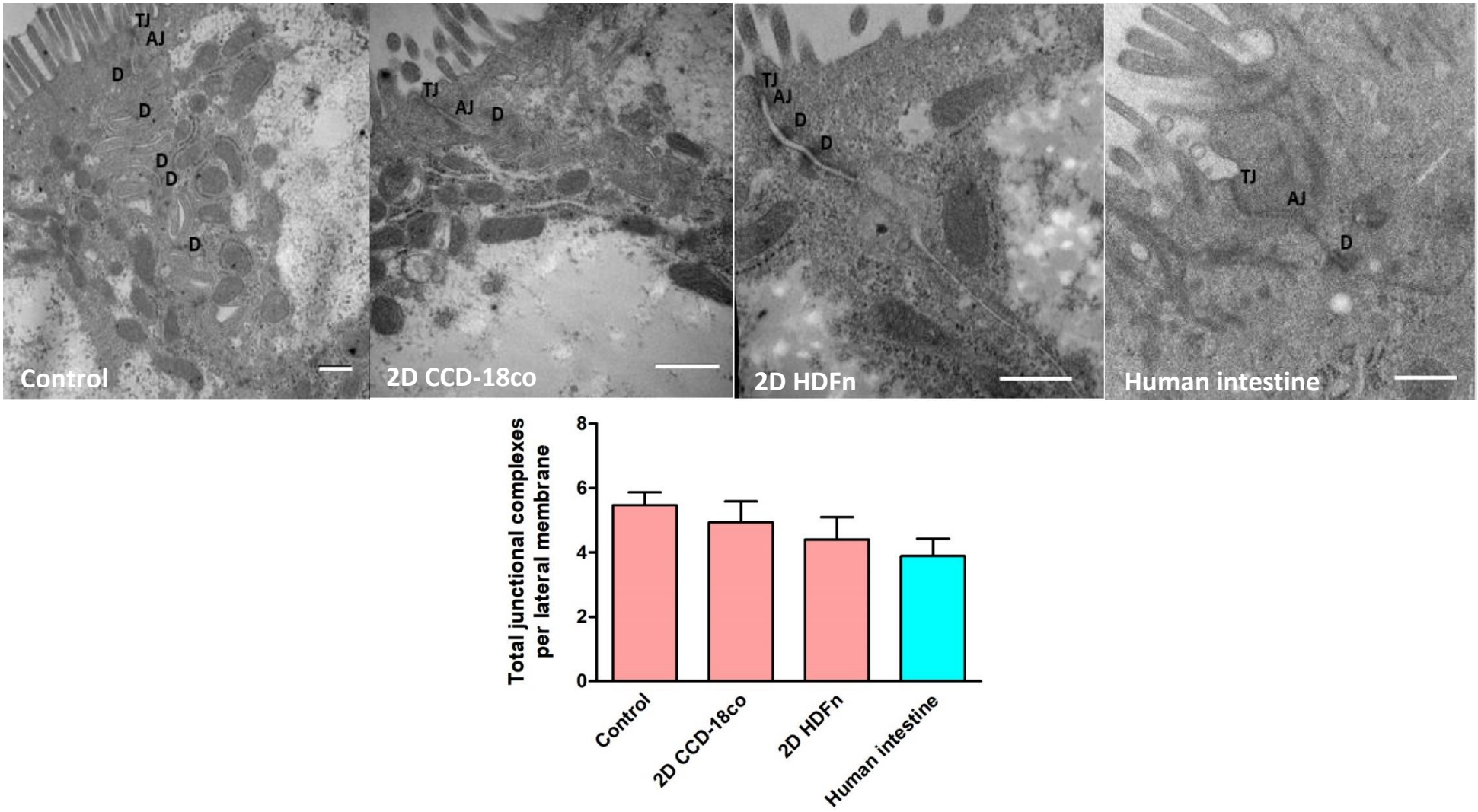

Figure 18: Analysis of the electron-dense junctional complexes expression. Junctional complexes expressed along the lateral membranes of Caco-2 cells in 2D models (n=15 cells for 3 independent samples) and small intestine tissue (n=10 cells from a single sample), were quantified from electron micrographs. Error bars represent the standard error of the mean (SEM). Even though it was observed a decrease in the number of junctional complexes expressed in paracrine effect models resembling human tissue results, it was not statistically significant for all the models and human tissue. TJ= tight junctions; AJ= adherens junctions; D= desmosomes. Scale bars: 0.5 µm.

To confirm those findings, an additional analysis of the expression of junctional proteins in 2D models was done by Western blot (figure 19). Proteins were extracted from cell lysates of paracrine effect and control models. β Actin and GAPDH were used as housekeeping proteins. The expression patterns showed a decrease in the expression of ZO-1, E-cadherin, occludin and claudin-1 junctional complexes proteins in the paracrine models treated with conditioned media derived from fibroblasts. As a way to quantify the expression of proteins from Western blot, it was performed a densitometry analysis (figure 20). Results revealed a decrease in the expression of all junctional complexes analysed in both 2D CCD-18co and 2D HDFn model.

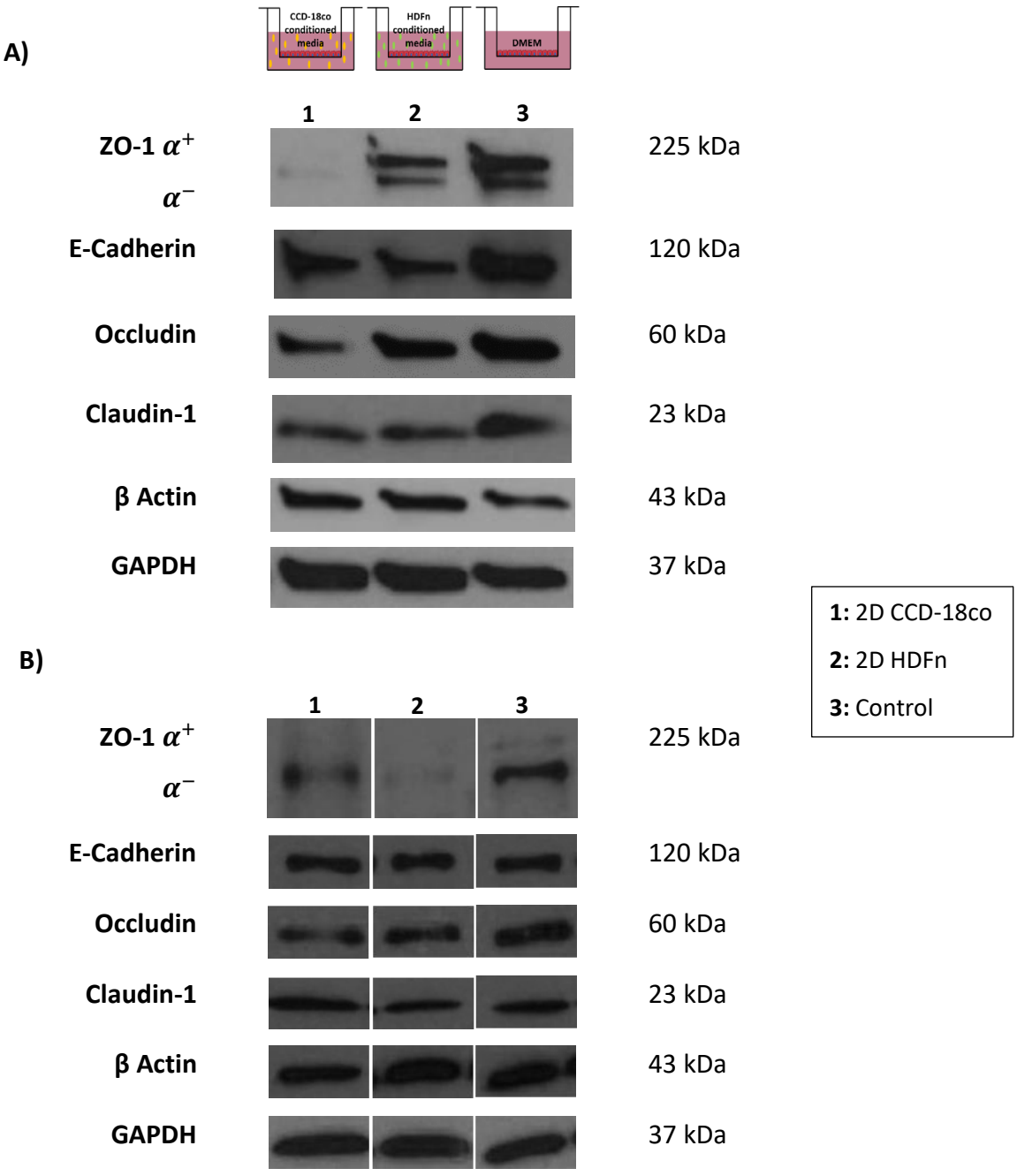

Figure 19: Western blot analysis of junctional protein expression in 2D models. A) Western blot analysis showed a decrease in all junctional complexes protein expression in paracrine effect models were observed in the bands. B) A second western blot was performed, and it was clearly observed a decrease in the expression of ZO-1 and occludin proteins.

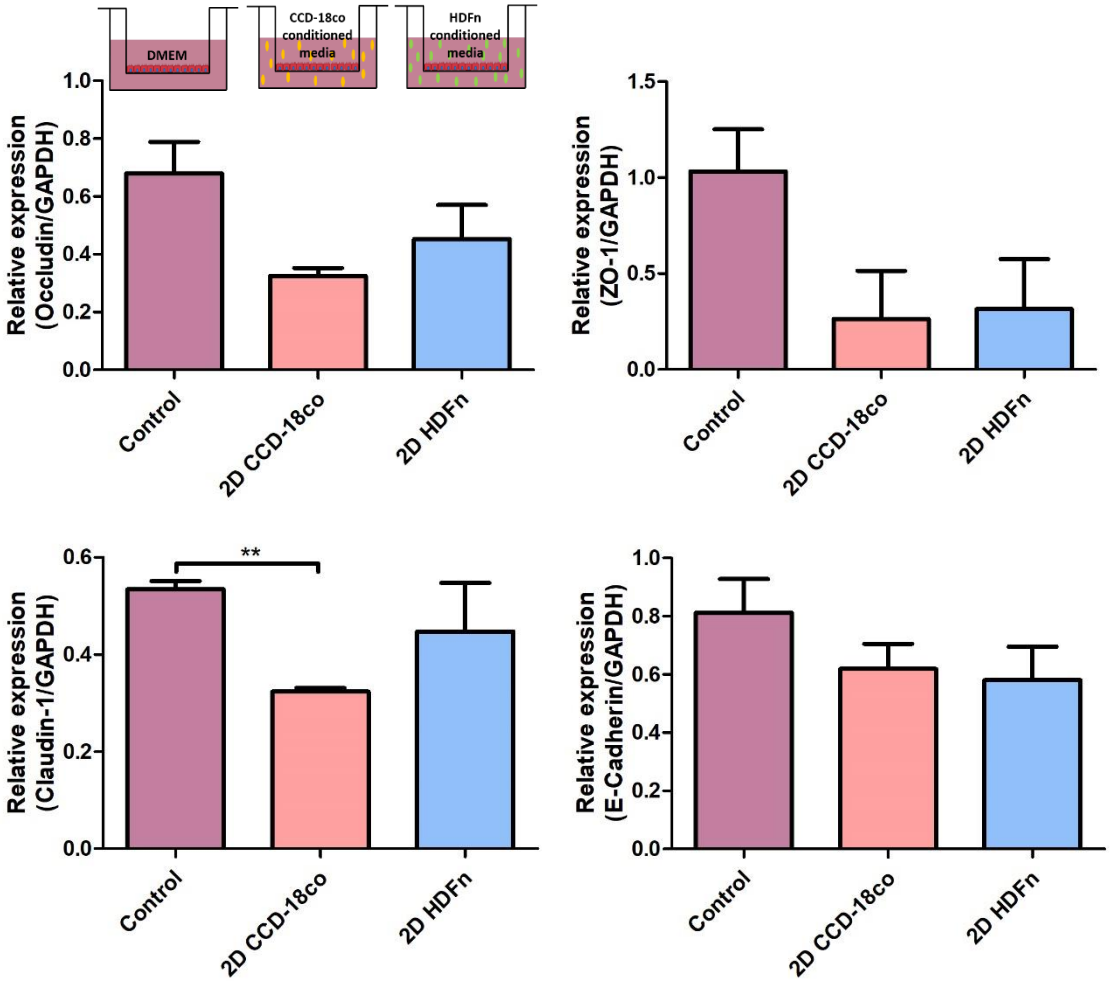

Figure 20: Densitometric analysis of junctional protein expression in 2D models. Variation in the protein expression from figure 19 was analysed by densitometry using the software Image J. Error bars represent the standard error of the mean (SEM), a total of n=2 independent samples. It was used GAPDH as the housekeeping protein. Results revealed a decrease in the expression of ZO-1, E-cadherin, occludin and claudin-1 proteins for both 2D CCD-18co and 2D HDFn models. T-test analysis revealed a significant reduction in the expression of claudin-1 in 2D HDFn paracrine model with P=0.0027.

3.3. 3D Cell Culture Models

3.3.1. Construction of 3D models and Caco-2 cells morphology

To study if there are morphology and physiology changes in Caco-2 cells when they are cultured in a 3D microenvironment, Caco-2 cells were seeded in co-culture with fibroblast cell lines using Alvetex® as the 3D scaffold. First, CCD-18co and HDFn were seeded and grown for 14 days within the scaffold and they were maintained with MEM and DMEM, respectively. More layers of CCD-18co fibroblasts were seeded on the days 7, 9 and 11 of culture.

After 14 days of fibroblast culture, Caco-2 cells were seeded on the 3D fibroblast culture and the models were maintained in DMEM to differentiate for 21 days. To note that in this work it was not included a 3D model of only Caco-2 cells grown on Alvetex®. The 3D co-culture models acquired a structure resembling native intestinal tissue. Caco-2 cells developed similar morphology to real tissue becoming significantly than those cultured in the conventional 2D environment (figure 21).

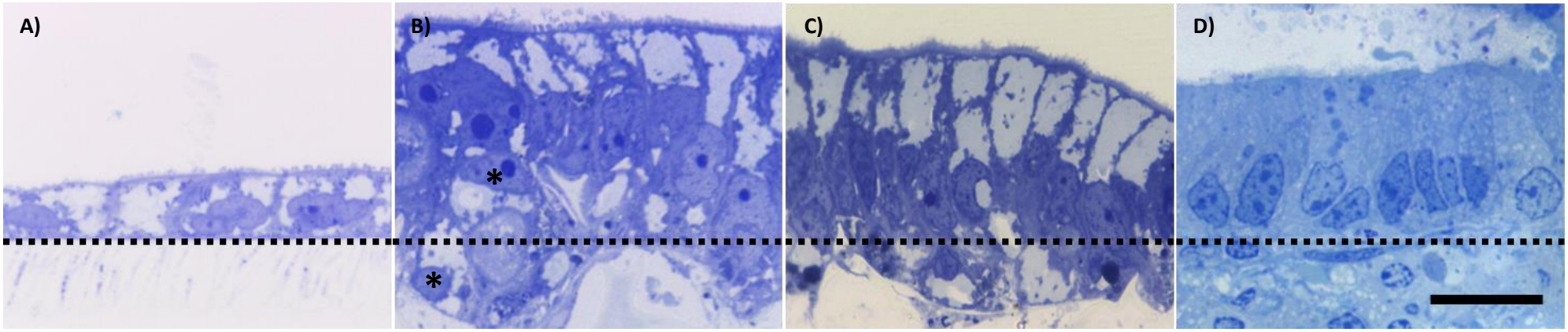

Figure 21: Changes in Caco-2 cells morphology in 3D models. Toluidine blue 0.5 µm sections of A) 2D Caco-2 cells cultured in Transwell® inserts and maintained with DMEM until differentiation; B) 3D CCD-18co: Caco-2 cells in co-culture with CCD-18co fibroblasts until differentiation, using Alvetex® as scaffold; C) 3D HDFn: Caco-2 cells co-cultured with HDFn fibroblasts until differentiation, using Alvetex® as scaffold; and D) Human intestine: normal human small intestine. Basement of epithelial cells is delimited with a non-continuous line. To state that figure 21A and 21D are the same as figure 10A and 10D, respectively and were included for comparison purposes. With exception of human tissue, it was taken images from at least 3 independent samples for each model; for human tissue it was taken images from a single sample A pair of asterisks indicate Caco-2 cell overlapping another Caco-2 cell. Scale bar: 10 µm.

Electron micrographs showed the presence of junctional complexes as dense features along the LPM. The presence of microvilli was observed in both 3D models (figure 22).

From the morphological analyses it was noted that when Caco-2 cells were co-cultured with CCD-18co and HDFn in Alvetex®, they extended their height, resembling the columnar shape observed in the native tissue. There was a clear difference in epithelial cell shape compared to the conventional 2D model when Caco-2 cells were grown on a Transwell® membrane.

Using ImageJ software, the heights and widths of single epithelial cells was recorded from electron micrographs (figure 23). The ratio between the height and width of a single epithelial cell was calculated. Results above the unit indicates that cells present an elongated shape, and below the unit, cells present a flattened shape. As expected, the quantified data showed that Caco-2 in co-culture with fibroblast cell lines in a 3D microenvironment better resemble the columnar shape of human intestine, in comparison with Caco-2 cells cultured in the conventional 2D microenvironment.

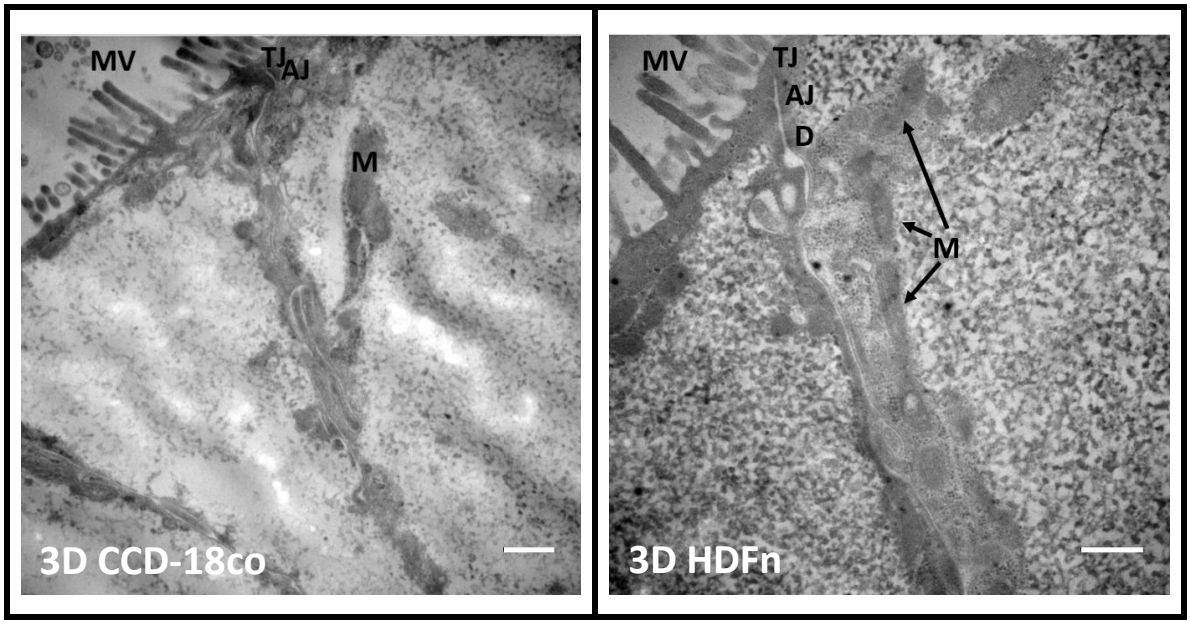

Figure 22: Ultrastructural features of Caco-2 cells in 3D models. At 21 days of Caco-2 cells culture, functional differentiation is defined by the appearance of junctional complexes and development of microvilli. TJ= tight junctions, AJ= adherens junctions, D= desmosomes, MV microvilli, M= mitochondria. Scale bars: 0.5µm.

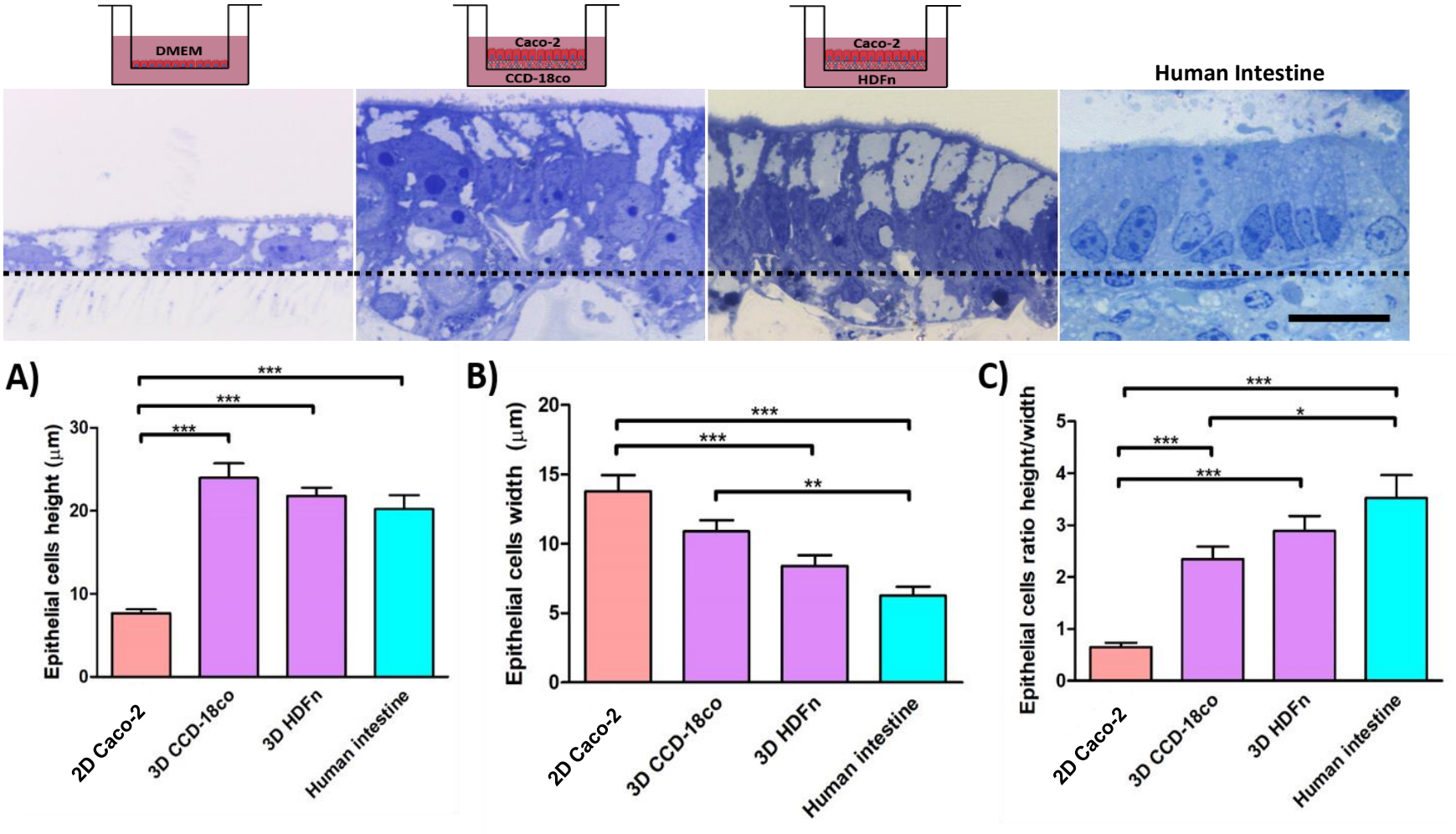

Figure 23: Morphometric analysis of epithelial cells in 3D models. A) Measurements of epithelial cells heights in 3D models; 2D caco-2 model; and human small intestine. B) Measurements of epithelial cells widths in 3D models; 2D caco-2 model; and human small intestine. C) Ratio between the height and width of epithelial cells in 3D models, 2D Caco-2 model and human small intestine. 2D caco-2 model and human intestine data in figure 23A, B and C are the same as in figure 12A, B and C, respectively. With exception of human intestine, 5 cells were measured from 3 different independent samples giving a total of n=15; for human intestine n=10 from a single sample. Error bars represent the standard error of the mean (SEM). It was run a One-way ANOVA analysis and Tukey Multiple Comparison Test ($P < 0.05$). To state that figure of toluidine blue sections represented above graphs is the same as figure 21 and were included in figure 23 for comparison purposes with the data. Analysis revealed that Caco-2 cells in novel 3D models present a columnar shape, resembling the epithelium in human small intestine. Scale bar= 10μm.

Ultrastructural observations of Caco-2 cells cultured in a more '*in vivo*-like' environment revealed that LPM resembled the elongated shape observed in human tissue, in contrast with the folded LPM in Caco-2 cells when they are cultured in a flat membrane (figure 24). In addition, there was a reduction in the electron-dense junctional complexes along the LPM of Caco-2 in the 3D models which was similar to that observed in the human intestine.

A)

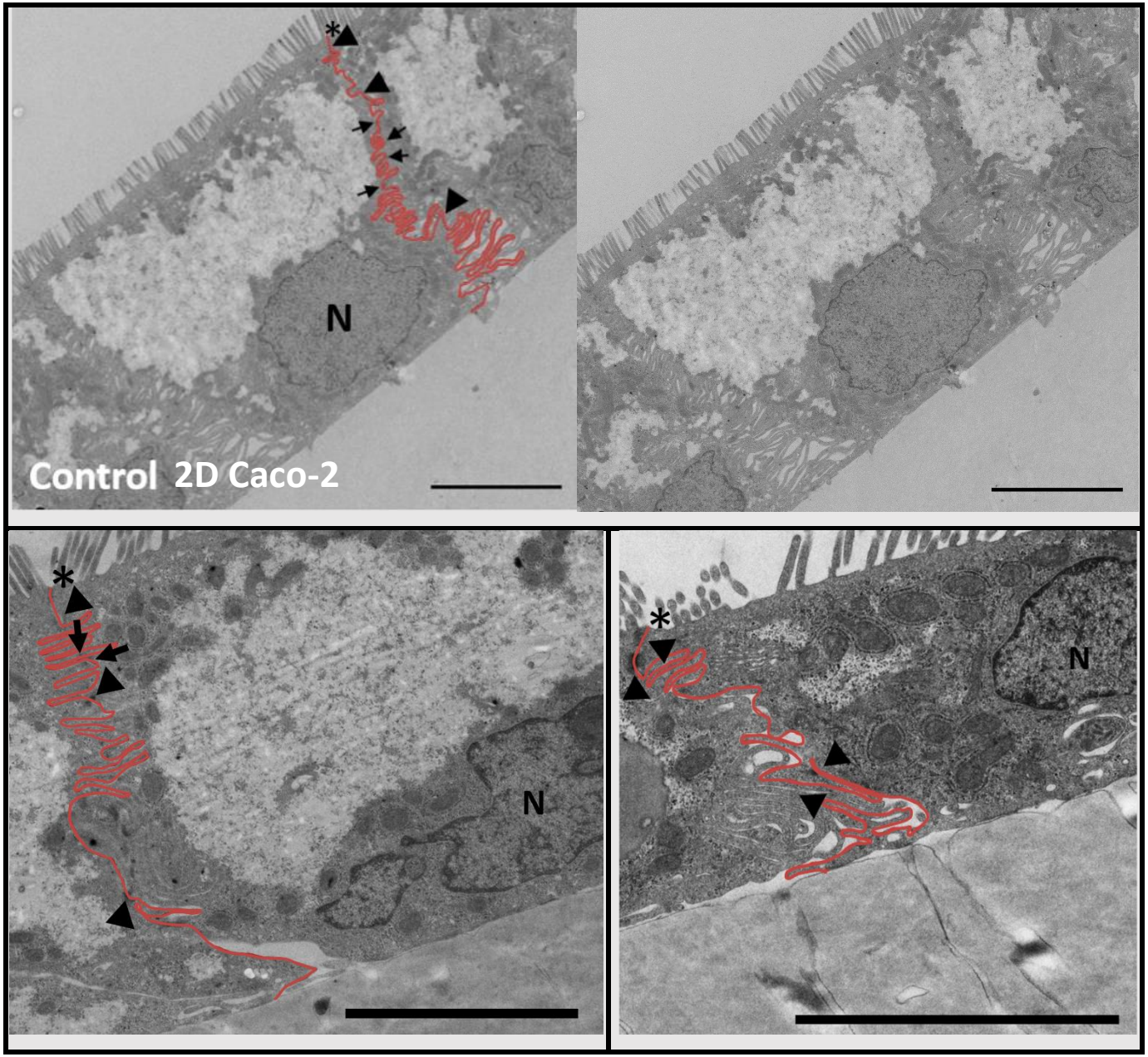

B)

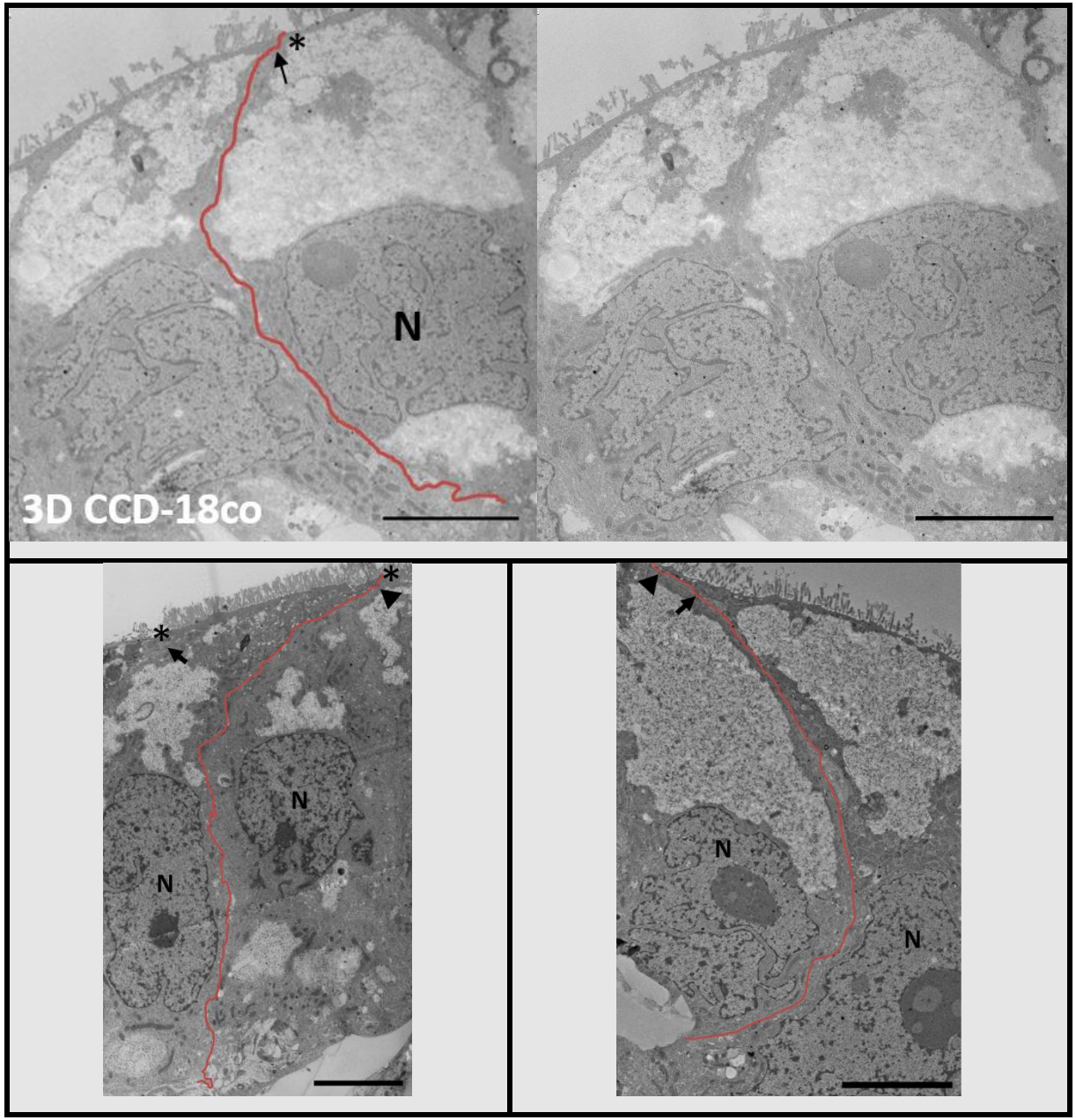

C)

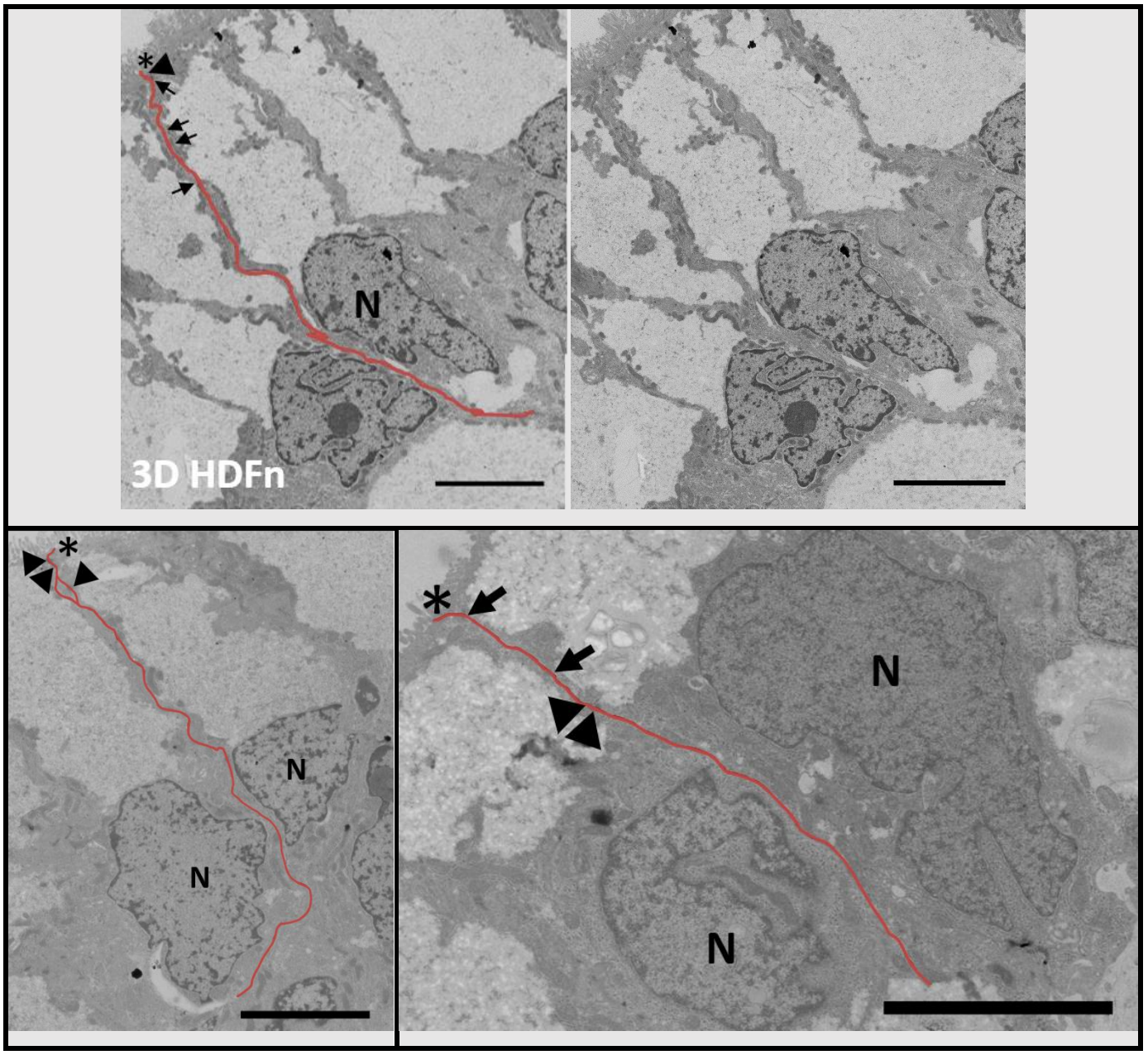

D)

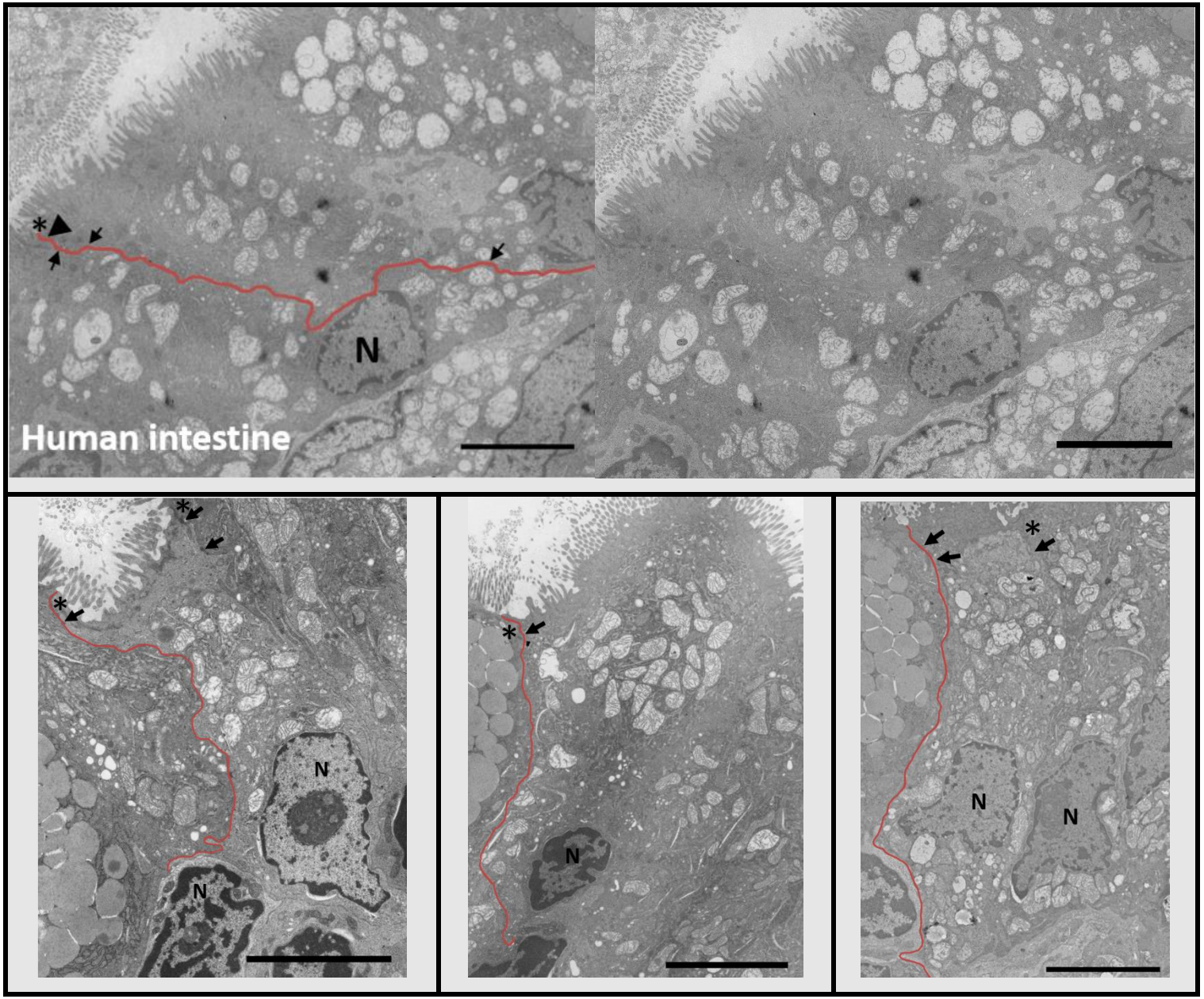

Figure 24: Electron micrographs of epithelial cells in 3D models. Electron micrograph of lateral membranes in 2D caco-2 model (A), 3D CCD-18co model (B), 3D HDFn model (C), and human small intestine (D). To state that figure 24A is the same as figure 13A. Epithelial lateral membranes are emphasised in salmon colour; tight junctions are indicated with asterisks; desmosomes with arrows; and adherent junctions with head arrows. N= nuclei, scale bars: 5 µm.

Subsequently, the length of the lateral membranes was measured in order to study the relationship between the LPM folding and cell height (figure 25 a, b). Results demonstrated that as 3D models presented less LPM length than conventional model, Caco-2 cells tend to be elongated and taller. Comparing those results in 2D and 3D models and native tissue, it could be said that decrease in the LPM folding is related to the increase in the epithelial cell height.

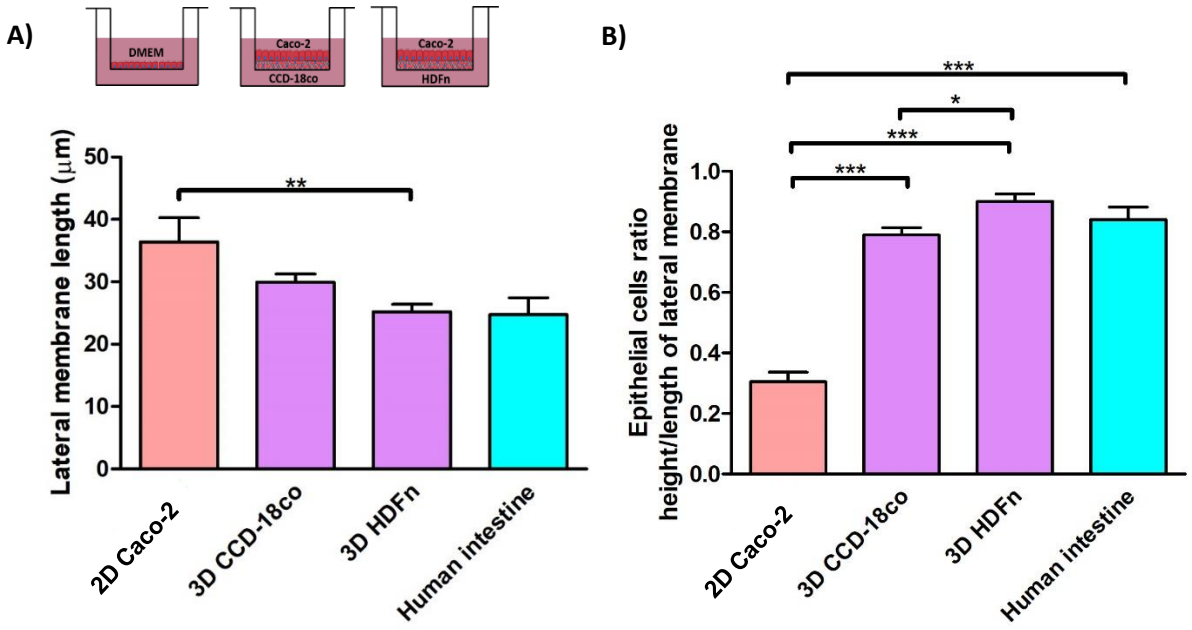

Figure 25: Morphometric analysis of epithelial cells lateral membranes in 3D models. A) Analysis of the epithelial lateral membrane lengths in 2D Caco-2 model and 3D models for n=25 cells measured for at least 3 independent samples; and in human small intestine for n=10 cells measured for a single sample. B) Ratio between the height and lateral membrane length of epithelial cells in 2D, 3D models and human small intestine. To state that 2D caco-2 model and human intestine data is the same as in figure 14. Error bars represent the standard error of the mean (SEM). An analysis One-way ANOVA demonstrated a significant variation of lateral membrane length among conditions with P=0.0065 (A) and P=0.0001 (B). A post hoc Tukey Multiple Comparison Test revealed that 3D HDFn model present a significant reduction at $P < 0.05$ in the lateral membrane length compared than 2D Caco-2 model.

3.3.2. mRNA expression of junctional complexes

Transcriptional analysis by qPCR experiment was run to study the changes of junctional proteins gene expression. mRNA was extracted at the end of culture for each model. Due to problems with the isolation of specific Caco-2 cells mRNA and contamination with fibroblast derived transcripts, it was proposed to use villin as reference gene. Villin is an actin-binding protein that is specifically found in the brush border of epithelial cells, which lead us to selectively study the gene expression

of Caco-2 cells in the diluted sample with fibroblasts mRNA. In order to confirm that fibroblast do not express villin, it was alongside run samples derived from fibroblasts only (figure 26). It was calculated the mRNA relative expression using the equation $2^{-\Delta\Delta Ct}$. A total of 3 independent samples or replicas were evaluated. Each replica was normalized to their respective control replica. At the end, control variance was calculated by choosing one replica and expressing the others as a relative proportion. As expected, it was demonstrated that cultures of fibroblasts do not express villin. However, it can be noticed that villin expression vary between all the models.

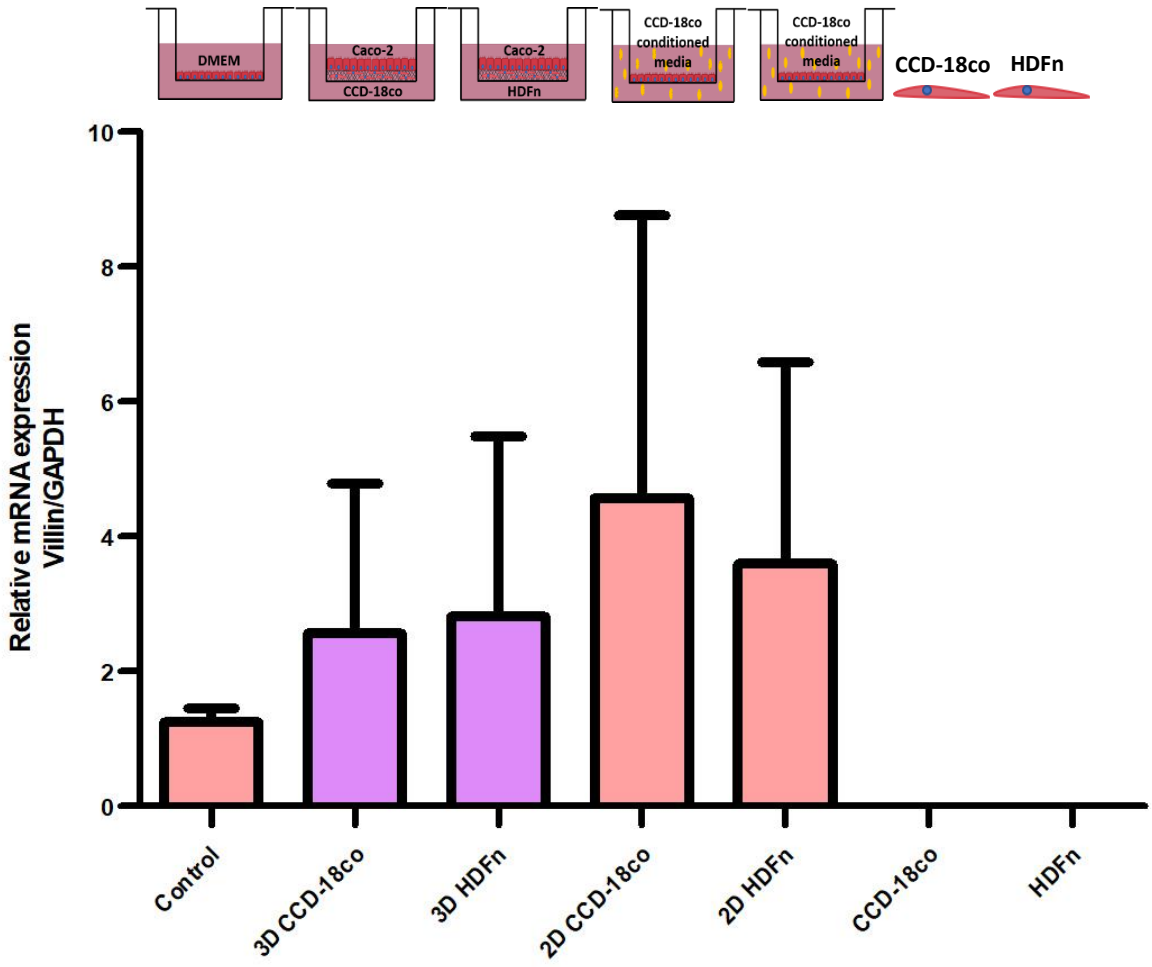

Figure 26: Villin mRNA expression in Caco-2 cells. Evaluation of the selectively expression of villin in Caco-2 cells demonstrated that fibroblasts lack of villin expression. 2D Caco-2 model was used as the control. Error bars represent the standard error of the mean (SEM), n=3 independent samples.

In order to assess junctional proteins gene expression in 3D models, villin was used as a reference gene. 2D models and untreated model results were also normalized with villin expression. One biological repeat was analysed from each experimental group in each test and the same control sample was loaded in all tests. A total of three tests were run to obtain data from three biological repeats. For each gene of interest, each cDNA sample was loaded for triplicate. mRNA relative expression was calculated using the equation $2^{-\Delta\Delta Ct}$. A total of 3 independent samples or replicas of each model and control were evaluated. Each model replica was normalized to their respective control replica. At the end, control variance was calculated by choosing one replica and expressing the others as a relative proportion. Results from 2D culture models were similar to the ones when it was used GAPDH as reference gene. In general, a decrease in the JC genes was observed compared to the untreated models. However, unexpected results were found in the 3D models with an observed upregulation of the occludin, ZO-1 and E-cadherin genes. Even though it is important to note that the variability in the expression of villin between the models, showed in figure 26, could be explained by villin expression in Caco-2 cells are unlike when they are growth in different microenvironments or conditions. This limitation may also affect the results in figure 27 making them not reliable to make inferences.

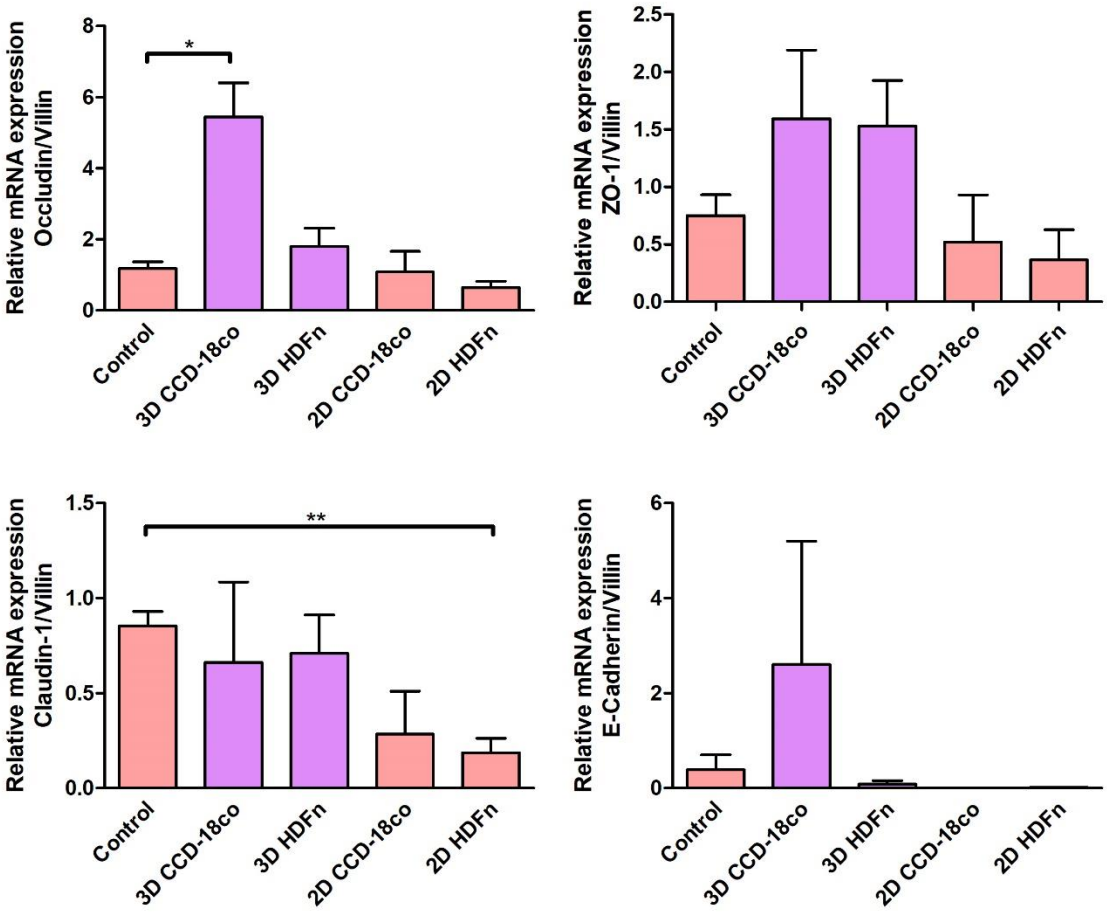

Figure 27: Analysis of the junctional proteins gene expression in 2D and 3D models using villin as reference gene. Variation in the gene expression of tight junction proteins (occludin, ZO-1 and Claudin-1) and adherens protein (E-Cadherin) in 2D and 3D models were analysed. 2D caco-2 model was used as the control. Error bars represent the standard error of the mean (SEM), n=3 independent samples. T-test analysis revealed a significant reduction in the expression of claudin-1 in 2D HDFn paracrine model with P=0.0035; and a significant upregulation of occludin in 3D CCD-18co model with P=0.0119. Analysis of this results revealed similarities with those in figure 16 for 2D paracrine effect models, using this time villin as reference gene. However, it was observed upregulation of occludin, ZO-1 and E-cadherin genes in 3D CCD-18co model; and occludin and ZO-1 genes in 3D HDFn model.

3.3.3. Protein expression of junctional complexes

Protein expression of junctional complexes in 3D models were analysed by immunohistochemistry. Samples were fixed in 1:1 methanol/acetone before being embedded in OCT compound. 7 µm sections of each model were immunostained against occludin, ZO-1, Claudin-1 and E-Cadherin junctional proteins (figure 28). Observations revealed a decrease in the intensity in all the junctional proteins analysed in the 3D models.

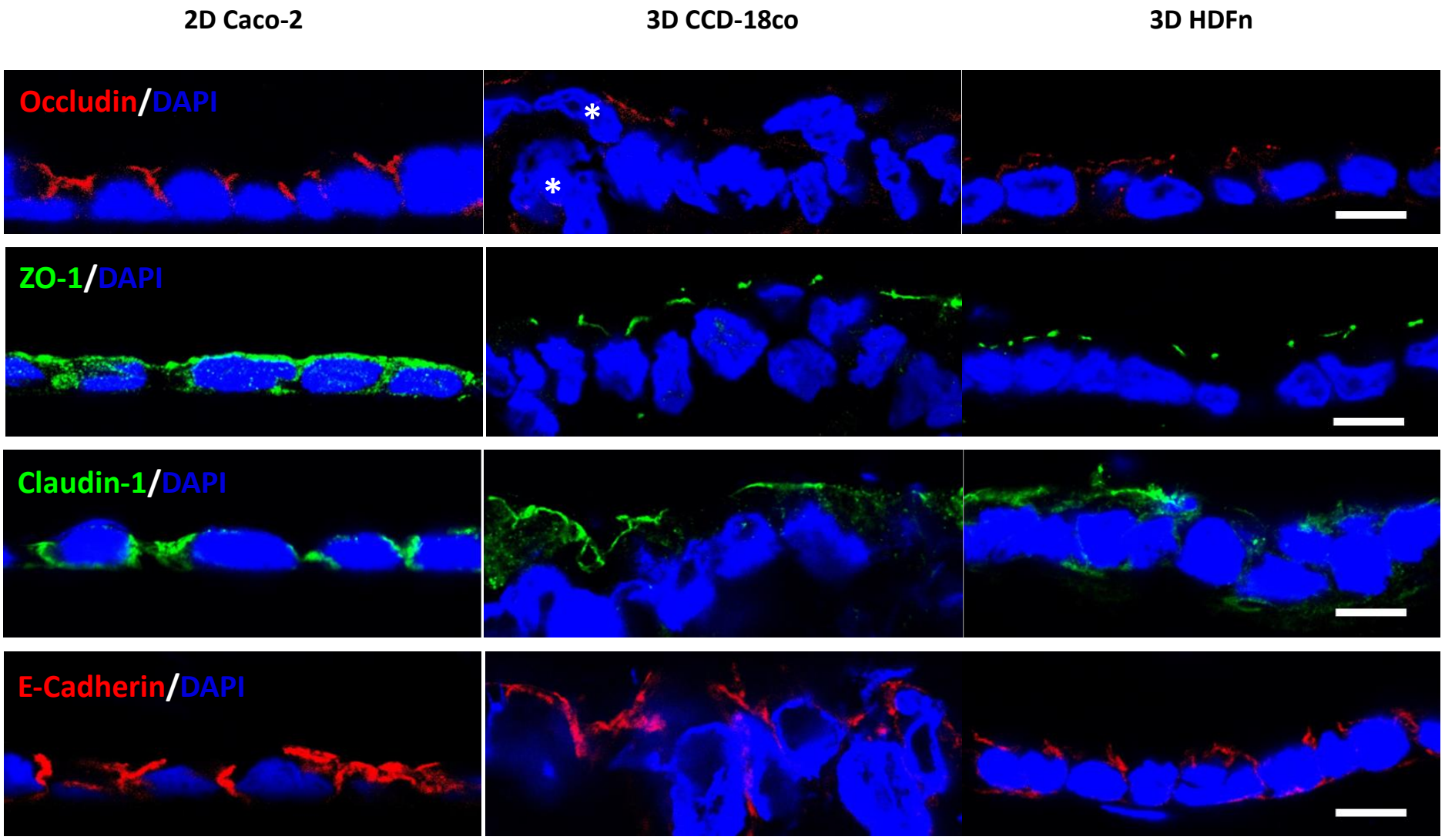

Figure 28: Immunofluorescence analysis of junctional proteins expression in 3D models. 3D intestinal models decrease the expression of Occludin, ZO-1, claudin-1 and E-cadherin proteins compared than conventional intestinal model. Confocal microscopy of Caco-2 cells co-cultivated with fibroblast cell lines in Alvetex® inserts for 21 days (3D CCD-18co and 3D HDFn) and 2D culture of Caco-2 cells cultivated in Transwell® insert for 21 days. OCT embedded sections fixed in 1:1 methanol/acetone were incubated with the primary antibody against junctional complexes, followed by the corresponding secondary antibody. Nuclei were counterstained with DAPI. To state that 2D Caco-2 model images in figure 28 are the same es in figure 17. A pair of asterisks indicate caco-2 cell overlapping another caco-2 cell. Pictures were taken from a single sample for each model. Scale bars: 10 µm.

Using TEM pictures, the total number of electron-dense features observed along the lateral membranes of 3D models was quantified and the results were compared to untreated models and human tissue (figure 29). Consistent with the immunostaining data, a reduction in the junctional complexes expression in the 3D models was observed compared to the 2D Caco-2 model.

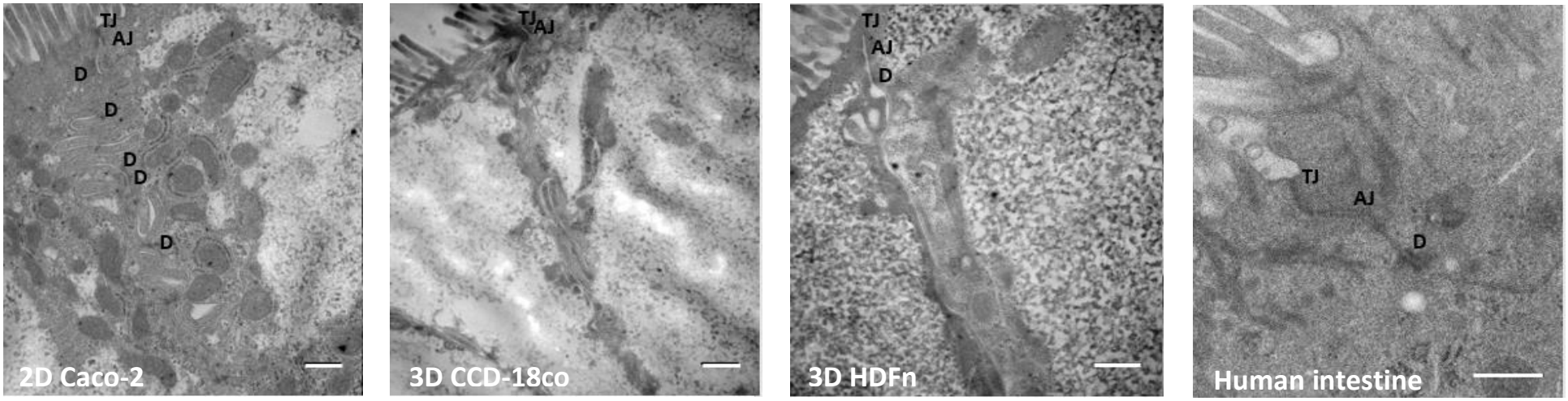

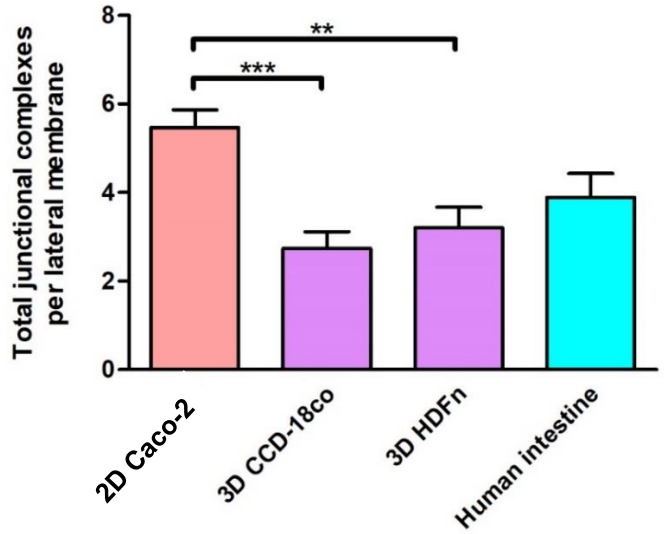

Figure 29: Analysis of electron-dense junctional complexes expression. Junctional complexes expressed along the lateral membranes of caco-2 cells in 2D model (n=15 cells for 3 independent samples), 3D models (n=15 cells for 3 independent samples) and small intestine tissue (n=10 cells from a single sample), were quantified from electron micrographs. Error bars represent the standard error of the mean (SEM). It was run a One-way ANOVA analysis and Tukey Multiple Comparison Test ($P < 0.05$). To state that images and data for 2D Caco-2 model and human intestine in figure 29 are the same as in figure 18. Analysis revealed a significant decrease in the expression of junctional proteins in 3D models in comparison with conventional 2D model and resembling human tissue. TJ= tight junctions; AJ= adherens junctions; D= desmosomes. Scale bars: 0.5 µm.

3.4. Morphology comparison of 2D and 3D models with human tissue

Lastly, it is important to highlight that the 3D microenvironment enhanced the intestinal structure of Caco-2 epithelial cells. As observed in the figure 22, Caco-2 cells acquired a more *in vivo* like morphology resembling the epithelium in the human small intestine when they are grown in direct co-culture with fibroblast cells on Alvetex® scaffold. Morphological comparisons demonstrated that when Caco-2 cells were cultured in a 2D microenvironment Transwell® membranes, their shape is shorter and wider than native tissue. However, Caco-2 cells were transformed when they were cultured in a 3D microenvironment, resembling the normal elongated shape with similar dimensions as those presented in the real human intestinal epithelium.

4. Discussion

The configuration of the junctional complexes along the lateral membrane is important for the characterisation of the cellular shape and function of epithelial cells. Changes in the structure of lateral surface are influenced by the surrounding environment. In this study, comparison of the intestinal lateral barrier structures and epithelial cells shapes were made between five *in vitro* intestinal models and human tissue. Caco-2 cells in a two-dimensional cell culture system were exposed to conditioned media derived from two different fibroblast cell lines: CCD-18co and HDFn, and their structure compared to untreated Caco-2 cells in the same 2D cell culture system. Additionally, Caco-2 cells in three-dimensional direct co-culture cell culture system with CCD-18co and HDFn fibroblast were also compared. Finally, human intestinal tissue samples were analysed and compared to all the models. The aim of the study is to create an intestinal *in vitro* model that better resembles the structure and function of native tissue.

4.1. Enhancement of Caco-2 model structure and function by indirect co-culture with fibroblast cells

4.1.1. Morphological changes

It is well documented in the literature that fibroblasts which form part of the intestinal mucosa, plays an important role in the regulation of epithelial cells maturation and behaviour. Cell-cell interactions between fibroblasts and epithelium are conducted through a paracrine mechanism mediated by growth factors (Visco *et al*., 2009). In an attempt to mimic these interactions, intestinal models have been created by culturing Caco-2 cells in indirect co-culture of fibroblast cell lines. This system consists of Caco-2 cells cultured with the fibroblast derived secretome consisting of growth factors, extracellular matrix and metabolites secreted into the media. Looking at the figure 10 it is distinguishable that Caco-2 cells tend to acquire different sizes throughout the membrane in all paracrine treated models and conventional model. Figure 12 confirmed that Caco-2 cells tend to be marginally thinner and taller under such growth conditions.

Analysis of higher magnification images (figure 13) revealed a significant morphological difference. Caco-2 cells in paracrine treated models developed lateral membranes that were less folded than those observed in the conventional 2D model. This was consistent with the structure of the lateral membrane in human tissue which were found to be more elongated. This could contribute to the

small changes in the cellular shape previously commented. There is no information from the literature reporting the mediator of this structural change. In this study it was hypothesized that this is due to changes in the expression of junctional complexes along the lateral membrane of Caco-2 cells in different *in vitro* models compared to native tissue. It was considered that junctional complexes would be expressed to a lesser degree than in the conventional 2D model, which itself does not closely resemble the structure of the human intestinal epithelium. A reduction in the expression of junctional complexes would in turn result in a decrease in the tightness of the barrier.

4.1.2. Decrease in TEER values in paracrine effect models correlated with the decrease in the lateral membranes folding

Transepithelial electrical resistance has been used as a method to study the integrity of the epithelial barrier. It has been observed that TEER values varies from laboratory to laboratory due to factors that can affect the measurement as the temperature, the time spent until stabilization of the measurement or the manage of the culture to the place of measurement. Even though, there is a markable tendency in the increase of those values in the conventional Caco-2 *in vitro* model after six days of culture. TEER values of paracrine treated models at the end of culture were found to more closely resemble those of native tissue, compared than the 2D Caco-2 model (Legen *et al*., 2005; Takenaka *et al*., 2014). These data further support the inconvenience of using the conventional 2D Transwell® model to predict novel drug absorption in human tissue as Caco-2 epithelial cells are too tight that do not enable a well-mediated transport. On the other hand, data reported in this study show that when Caco-2 cells were co-cultured using conditioned media from fibroblasts, lateral membrane folding decreased compared to the conventional 2D counterpart. These observations correlated with the epithelial resistance findings where epithelial cells decreased their TEER values and there was a reduction in lateral membrane folding. Such differences also support the idea that lateral membrane structure depends on the degree of the tight junction proteins expression. In other words, paracrine treated models developed less folded lateral membranes due to the presence of less complex epithelial barrier than those presented in the conventional 2D model.

Additionally, an interesting observation from the TEER results may be considered for future studies. TEER values from the 18th to the 21st day of culture remained similar in the 3 different models. This might suggest that Caco-2 cells reached maturation around the 18th day. Hence, time of culturing and building the intestinal model could decrease leading to a reduction of costs and time. However,

it will be necessary to further evaluate the maturation of models by microscopy and molecular analysis to confirm the models are sufficiently differentiated after 18 days of culture.

4.1.3. Changes in gene expression of junctional complexes

RT-qPCR analysis of paracrine treated models revealed downregulation of occludin and claudin 1 genes which encode tight junction proteins. Occludin is expressed to a greater degree than the other tight junction genes analysed. This observation was also reported when monolayer Caco-2 cells were cultured for 6, 12 and 19 days suggesting occludin as a major participant in the formation of tight junctions (Matsusaki *et al*., 2015; Orlando *et al*., 2014). Occludin interact with tight junction associated proteins such as ZO-1, ZO-2, JAMs, among others and this may also explain their importance in the regulation of tight junction proteins (Feldman *et al*., 2005).

It is well documented in the literature that untreated Caco-2 monolayer models have limitations and cells form a more complex and tighter barrier than epithelial cells found in the human intestine (Sun *et al.*, 2008). Results obtained from the comparison of the gene expression of junctional complexes suggest that both CCD-18co and HDFn fibroblasts regulate the barrier function of Caco-2 cells. This is carried out by mediating the expression of tight junction genes at levels that may improve the expression of those proteins in the lateral membranes. However, analysis at protein levels will be discussed thereafter with the intention to strengthen those findings.

It was also observed a decrease in the expression of E-cadherin gene in the paracrine effect models. Downregulation of this adherens junction gene correlate with the TEER results. A study by Guo *et al*. (2003) inhibited the expression of E-cadherin in normal intestinal epithelial cells (IEC-6 line) and as a result, the paracellular permeability was increased. This was consistent with the proposal that E-cadherin have a main role in the integrity of epithelial cells barrier.

4.1.4. Changes in protein expression of junctional complexes

Examination of the immunofluorescent images confirmed the downregulation in the expression of occludin, ZO-1, claudin-1 and E-cadherin proteins in the paracrine effect models. All four junctional complexes tested observed a decrease in their expression in the paracrine treated models: with ZO-1 expression showing the greatest reduction. Z-sections images were helpful in identifying the immunofluorescence localization of those junctional complexes in the lateral membrane of Caco-2 cells. However, image data of paracrine treated models show that claudin-1 expression does not clearly appear to be localized in the lateral membrane as it was observed in the other models. The

most likely explanation is a technical issue where the OCT blocks of the specimens were not properly aligned with the blade during cryostat sectioning and that is why some nuclei were observed behind others.

Electron micrographs were used as a way to quantify the expression of junctional complexes in Caco-2 cells. It was quantified the number of electron-dense features observed per lateral membrane was consistent with the immunofluorescent data. The conventional 2D Caco-2 model had the greater number of junctional complexes recorded from image analysis. Human small intestinal tissue was also quantified and contained the lowest number of electron-dense features.

Additionally, western blot analysis was found to also be consistent with the previous protein assessments. Even though, it was observed an upregulation of ZO-1 gene expression while at protein level it was observed a downregulation. One explanation of this behaviour is that some studies have stated that not all total mRNAs in the cell will translate into proteins, and there are post-translational modifications or degradation that could occur (Gry *et al*., 2009; Maier *et al*., 2009). Looking at the expression of ZO-1 protein, it was obtained two bands during the immunolabelling close to the 225 kDa which is the expected molecular weight for the antibody used. The appearance of two bands could be explained by the recognition of the epitopes of two different isoforms because it was used a polyclonal antibody. It has been reported that the ratio in the expression of α^{+}/α^{-} isoforms of ZO-1 in Caco-2 cells increases in parallel with increased level of cell differentiation (Ciana *et al*., 2010). Results confirmed Caco-2 cells were well differentiated at the end of culture. CCD-18co paracrine treated models expressed ZO-1, occludin and claudin-1 proteins at a lower level compared to the other models. Nonetheless, in the HDFn paracrine treated model a reduction in expression was also observed compared than the conventional 2D model. The expression of E-cadherin also reduced similarly in the paracrine treated models. These results correlate with those obtained at gene level. It is important to notice how E-cadherin expression correlates with the presence of tight junctions expression. In accordance with Tunggal *et al*. (2005), this adherens junction protein has a main role during tight junction formation involving a signalling mechanism. The data presented herein suggest that the CCD-18co and HDFn secretome does have an effect in the maturation of the epithelial barrier resulting in an epithelial structure that more closely resembles human intestinal tissue.

4.2. Novel intestinal 3D models in a direct co-culture system produce a morphology and physiology more relevant to native intestinal tissue

4.2.1. Caco-2 cells cultured in novel 3D models show improved morphology compared than conventional 2D models

Recent studies have reported differences in the morphology and function of cells when they are grown on a flat surface or in a 3D microenvironment that enable the cells acquire a more *in vivo*-like structure (Baker & Chen, 2012). With the intention of creating an *in vitro* model that better resembles the structure of human intestinal mucosa, Caco-2 cells were grown in direct co-culture with CCD-18co or HDFn fibroblast cell lines using Alvetex® technology. Fibroblasts were put in culture within the scaffold for 14 days. Then, Caco-2 cells were growth for 21 days on the scaffold in co-culture with the fibroblasts. After the 35 days of culture, the morphology of the models was analysed. It was demonstrated that Caco-2 in 3D models developed characteristics of a columnar epithelium. Electron microscope images clearly showed the development of microvilli conforming the brush border and junctional complexes that constitute the lateral barrier. Toluidine blue histological sections were useful to demonstrate the anatomy of the model showing a layered cellular structure. When comparisons with the human intestinal tissue were made, the similarity in terms of structure was evident between the *in vitro* models when Caco-2 were co-cultured with fibroblasts in a 3D microenvironment. Epithelial cells in both types of 3D models developed dimensions that approximate those of epithelial cells in native tissue. As demonstrated above, fibroblast had a positive effect in the development of Caco-2 when they were cultured in a plane substrate or membrane. However, these findings support the notion that phenotype and physiology of Caco-2 might be enhanced by the more *in vivo*-like microenvironment where direct cell-cell contact is made, recapitulating the structure of the normal intestinal mucosa.

Further analysis at higher magnification showed that Caco-2 cells in 3D models presented more elongated lateral membranes. From the results obtained in the ratio between the epithelial height and length of lateral membrane it could be inferred that as the cells got taller, lateral membranes decreased their folding as observed in the conventional 2D model. It can not be ascribed these changes only to the naturality of the culture system (2D or 3D) because there is more than one factor that can vary Caco-2 cells behaviour. To mention some of them, the seeding density impact in the time of culture until cell differentiation (Ferrec *et al*., 2001), the medium composition *(Li et*

al., 2004; Perdikis *et al*., 1998), the paracrine factor as the model used for comparison consisted of a 2D culture of Caco-2 cells alone, and the material and pore size of the support (Behrens & Kissel, 2003). Even though, observations from the 3D models evaluated were compared and showed to be consistent with human intestinal tissue demonstrating their resemblance.

4.2.2. Changes in gene expression of junctional complexes exhibited differences compared to the conventional 2D models

Turning now to the molecular analysis, total mRNA was extracted from the models in order to study the expression of junctional complexes. One concern about the extraction of total mRNA to analyse gene expression in Caco-2 cells was that samples were diluted with mRNA from the fibroblasts. To calculate the relative mRNA expression, it would be necessary to normalise results to a reference gene. Considering that well established reference genes are expressed, by its nature, for both Caco-2 and fibroblast cell lines, results would not be representative. Due to time constraints, it was not possible to obtain sufficient quantities of mRNA from isolated Caco-2 cells (e.g. as could be achieved by laser capture microscopy) in order to proceed with the RT-qPCR analysis. Nonetheless, the most feasible solution to this issue was to use villin as housekeeping gene with the total mRNA extracted from the models. Villin is a cytoskeletal protein that is specifically localised in the microvilli of epithelial cells and it has been used in other studies to selectively estimate gene expression in Caco-2 (Matsusaki *et al*., 2015). To prove that only epithelial cells express this protein, it was analysed by RT-qPCR mRNA of the conventional model, both 3D models and fibroblast only cell cultures. The results demonstrated that only Caco-2 expressed villin which was non-detectable in samples derived from fibroblasts.

Some unexpected results were found when examining the expression of genes encoding junctional complexes. It was observed upregulation of occludin, ZO-1 and E-cadherin genes in the 3D CCD-18co model. Whilst claudin-1 was found slightly reduced. In the 3D HDFn model, occludin and ZO-1 genes were more expressed than in the conventional model. Claudin-1 gene was expressed similar as the control and downregulation was observed for E-cadherin gene. By the fact that downregulation and upregulation of certain junctional complexes were found, it could be thought that the use of villin as reference gene may have been inaccurate. However, expression of all junctional complexes in the 2D models were afterwards normalised to this gene and results, excepting for ZO-1 gene, behaved similar like when GAPDH was used as reference gene. Even though there is still a concern about some variation that could be in the total mRNA for villin between 3D and 2D constructs. It is

known Caco-2 cells behaviour is influenced by the microenvironment surrounded and additional studies should be done in order to assess and compare the expression of villin protein when they are grown in different conditions. That being said, there is another limitation when conventional 2D Caco-2 model is used as control. Caco-2 cells growth are influenced by the filter support as it was demonstrated in the morphologic analysis and it could also be presented functional differences. Additionally, functional changes may be influenced also by the medium composition (Li *et al*., 2004; Perdikis *et al*., 1998). Nevertheless, additional analyses were subsequently performed at protein level.

4.2.3. Changes in protein expression of junctional complexes

Immunofluorescent data demonstrated protein expression of junctional complexes in the 3D models. Z-sections of each of the 3D constructions were immunolabeled with antibodies for occludin, ZO-1 and Claudin-1 tight junctions; and for E-cadherin adherens junction. When pictures were compared than the conventional 2D model pictures it was noticed that expression of occludin and ZO-1 tight junctions proteins decreased remarkably in both 3D CCD-18co and 3D HDFn models. Even though claudin-1 and E-cadherin proteins expression outcome is not immediately obvious, it was also observed a decrease in their expression in both novel 3D constructions. In addition, it could be observed Caco-2 cells overlapping with others in the 3D CCD-18co model and this is most likely a technical issue concerning histology sample preparation as explained earlier.

Quantification of junctional complexes along the lateral membrane produced some interesting findings. There was a significant decrease in the junctional features quantified in both 3D CCD-18co and 3D HDFn mucosal models compared to the conventional 2D model. These reductions were greater than the number of junctional features quantified in the human intestinal tissue. Based on the mRNA levels observations, it was thought that protein expression would have the same behaviour: increased expression of occludin, ZO-1 and E-cadherin in the 3D CCD-18co model, and ZO-1 in the 3D HDFn model. However, there is some concern as to whether mRNA levels correlate with the protein levels and most importantly, the use of villin that may not be a reliable reference gene. Moreover, as previously mentioned, not all total mRNAs in the cell will translate into proteins, and there are post-translational modifications or degradation that could occur (Gry *et al*., 2009; Maier *et al*., 2009).

It is unfortunate that this aspect of the project did not include a molecular method, such as western blot, to further analyse the expression of the proteins being studied. Nonetheless, there is

compelling evidence from the immunofluorescence and electron microscopy data that showed there was a downregulation in the appearance of electron dense junctional complexes and decreased protein expression of occludin, ZO-1 and Claudin-1 tight junctions, and E-cadherin adherens junctions. Additionally, protein expression results could be compared in futures studies with the human intestine in order to assess their resemblance.

5. Conclusion and Further Directions

This research has shown that human colon normal fibroblasts and neonatal human dermal fibroblasts provides an environment that enhance human colorectal adenocarcinoma cells to develop a more tissue-like structure and alter their lateral barriers. 2D Caco-2 monolayer model is extensively used but have limitations in the prediction of human small intestine behaviour during permeability assays. The findings in this study have provided evidence that fibroblast signalling can modulate molecular mechanisms in Caco-2, changing their barrier properties. Expression of occludin, ZO-1 and claudin-1 tight junctions, and E-cadherin adherens junction decreased in both mRNA and protein levels. Those changes were important to maintain the lateral membrane integrity resembling the native tissue. The second major finding was that growth conditions in both 3D intestinal models proposed in this work contributed epithelial cells to develop more relevant phenotype and physiology.

Inconsistencies in some mRNA tight junction expression in 2D paracrine effect models that did not reflect the protein levels results could be attributed to potential post-translational modifications. Results from the junctional complexes gene expression analysis for 3D models were not reliable due to the limitation previously discussed on the use of villin as reference gene. Also, it was not possible in this study to perform further protein analysis to the 3D models to endorse microscopy analysis and it would be interesting to further assess protein expression by western blot analysis.

Furthermore, notwithstanding epithelial cells in 3D models presented morphological dimensions close to the native tissue, improvements in the 3D constructions could be achieved by further increasing the complexity of the tissue model by adding additional cell types such as endothelial cells or immune cells. This might be of interest to seek in a future work keeping in mind the main goal to recreate a more relevant *in vitro* model.

6. Bibliography

Baker, B. M., & Chen, C. S. (2012). Deconstructing the third dimension – how 3D culture microenvironments alter cellular cues. *Journal of Cell Science*, *125*(13), 3015–3024. https://doi.org/10.1242/jcs.079509

Behrens, I., & Kissel, T. (2003). D o cell culture conditions influence the carrier-mediated transport of peptides in Caco-2 cell monolayers ? *European Journal of Pharmaceutical Sciences*, *19*, 433–442.

Borchardt, R. T. (1989). Characterization of the Human Colon Carcinoma Cell Line (Caco-2) as a Model Permeability. *GASTROENTEROLOGY*, *96*(3), 736–749.

Braun, A., Hammerle, S., Suda, K., Rothen-rutishauser, B., Gunthert, M., Kramer, S. D., & Wunderli-allenspach, H. (2000). Cell cultures as tools in biopharmacy. *European Journal of Pharmaceutical Sciences*, *2*(11), 51–60.

Briske-anderson, M. J., Finley, J. W., Newman, S. M., & Newman, M. (1997). Experimental Biology and Medicine. *Exp Biol Med*, *214*(3), 248–257. https://doi.org/10.3181/00379727-214-44093

Ciana, A., Meier, K., Daum, N., Gerbes, S., Veith, M., Lehr, C., & Minetti, G. (2010). A dynamic ratio of the α^{+} and α^{-} isoforms of the tight junction protein ZO-1 is characteristic of Caco-2 cells and correlates with their degree of differentiation. *Cell Biology International*, *34*(6), 669–678. https://doi.org/10.1042/CBI20090067

Collins, J., & Bhimji, S. (2017). *Anatomy, Abdomen, Small Intestine*. Treasure Island (FL): StatPearls.

Dosh, R. H., Essa, A., Jordan-Mahy, N., Sammon, C., & Le Maitre, C. L. (2017). Use of hydrogel scaffolds to develop an in vitro 3D culture model of human intestinal epithelium. *Acta Biomaterialia*, *62*, 128–143. https://doi.org/10.1016/j.actbio.2017.08.035

Dowling, P., & Clynes, M. (2011). Conditioned media from cell lines: A complementary model to clinical specimens for the discovery of disease-specific biomarkers. *Proteomics*, *11*(4), 794–804. https://doi.org/10.1002/pmic.201000530

Ebnet, K. (2008). Organization of multiprotein complexes at cell-cell junctions. *Histochemistry and Cell Biology*, *130*(1), 1–20. https://doi.org/10.1007/s00418-008-0418-7

Edmondson, R., Broglie, J. J., Adcock, A. F., & Yang, L. (2014). Three-Dimensional Cell Culture Systems and Their Applications in Drug Discovery and Cell-Based Biosensors. *ASSAY and Drug Development Technologies*, *12*(4), 207–218. https://doi.org/10.1089/adt.2014.573

Elamin, E., Jonkers, D., Juuti-Uusitalo, K., van IJzendoorn, S., van IJzendoorn, S., Troost, F., … Masclee, A. (2012). Effects of ethanol and acetaldehyde on tight junction integrity: In vitro study in a three dimensional intestinal epithelial cell culture model. *PLoS ONE*, *7*(4). https://doi.org/10.1371/journal.pone.0035008

Feldman, G. J., Mullin, J. M., & Ryan, M. P. (2005). Occludin: Structure, function and regulation. *Advanced Drug Delivery Reviews*, *57*(6), 883–917. https://doi.org/10.1016/j.addr.2005.01.009

Ferrec, E. Le, Chesne, C., Artusson, P., Brayden, D., Fabre, G., Gires, P., … Rousset, M. (2001). In Vitro Models of the Intestinal Barrier. *ECVAM Workshop 46*, *29*, 649–668.

Gèoke, M., Kanai, M., & Podolsky, D. K. (1998). Intestinal fibroblasts regulate intestinal epithelial cell proliferation via hepatocyte growth factor. *American Journal of Physiology*, *274*(5 Pt 1), G809-18.

González-Mariscal, L., Miranda, J., Raya-Sandino, A., Domínguez-Calderón, A., & Cuellar-Perez, F. (2017). ZO-2, a tight junction protein involved in gene expression, proliferation, apoptosis, and cell size regulation. *Annals of the New York Academy of Sciences*, *1397*(1), 35–53. https://doi.org/10.1111/nyas.13334

Gry, M., Rimini, R., Strömberg, S., Asplund, A., Pontén, F., Uhlén, M., & Nilsson, P. (2009). Correlations between RNA and protein expression profiles in 23 human cell lines. *BMC Genomics*, *10*, 1–14. https://doi.org/10.1186/1471-2164-10-365

Guo, X., Rao, J. N., Liu, L., Zou, T.-T., Turner, D. J., Bass, B. L., & Wang, J.-Y. (2003). Regulation of adherens junctions and epithelial paracellular permeability: a novel function for polyamines. *American Journal of Physiology-Cell Physiology*, *285*(5), C1174–C1187. https://doi.org/10.1152/ajpcell.00015.2003

Hartsock, A., & Nelson, W. J. (2008). Adherens and Tight Junctions: Structure, Function and Connection to the Actin Cytoskeleton. *Biochim Biophys Acta*, *1778*(3), 660–669. https://doi.org/10.1016/j.bbamem.2007.07.012.Adherens

Hay, M., Thomas, D. W., Craighead, J. L., Economides, C., & Rosenthal, J. (2014). Clinical development success rates for investigational drugs. *Nat Biotech*, *32*(1), 40–51. https://doi.org/10.1038/nbt.2786\rhttp://www.nature.com/nbt/journal/v32/n1/abs/nbt.2786.html#supplementary-information

Hoffmann, O. I., Ilmberger, C., Magosch, S., Joka, M., Jauch, K. W., & Mayer, B. (2015). Impact of the spheroid model complexity on drug response. *Journal of Biotechnology*, *205*, 14–23. https://doi.org/10.1016/j.jbiotec.2015.02.029

Jeong, D., Han, C., Kang, I., Park, H. T., Kim, J., Ryu, H., … Park, J. (2016). Effect of concentrated fibroblast-conditioned media on in vitro maintenance of rat primary hepatocyte. *PLoS ONE*, *11*(2), 1–14. https://doi.org/10.1371/journal.pone.0148846

Jung, P., Sato, T., Merlos-suárez, A., Barriga, F. M., Iglesias, M., Rossell, D., … Batlle, E. (2011). Isolation and in vitro expansion of. *Nature Medicine*, *17*(10), 1225–1227. https://doi.org/10.1038/nm.2470

Kauffman, A. L., Gyurdieva, A. V., Mabus, J. R., Ferguson, C., Yan, Z., & Hornby, P. J. (2013). Alternative functional in vitro models of human intestinal epithelia. *Frontiers in Pharmacology*, *4 JUL*(July), 1–18. https://doi.org/10.3389/fphar.2013.00079

Khanna, I. (2012). Drug discovery in pharmaceutical industry: Productivity challenges and trends. *Drug Discovery Today*, *17*(19–20), 1088–1102. https://doi.org/10.1016/j.drudis.2012.05.007

Kim, G., Ginga, N. J., & Takayama, S. (2018). Integration of Sensors in Gastrointestinal Organoid Culture for Biological Analysis. https://doi.org/10.1016/j.jcmgh.2018.03.002

Knight, E., & Przyborski, S. (2015). Advances in 3D cell culture technologies enabling tissue-like structures to be created in vitro. *Journal of Anatomy*, *227*(6), 746–756. https://doi.org/10.1111/joa.12257

Kowalczyc, A. P., Green, K. J., Kowalczyk, A. P., & Green, K. J. (2013). Structure, Function and Regulation of Desmosomes. *National Institutes of Health*, *116*, 95–118. https://doi.org/10.1016/B978-0-12-394311-8.00005-4.Structure

Legen, I., Salobir, M., & Kerč, J. (2005). Comparison of different intestinal epithelia as models for absorption enhancement studies. *International Journal of Pharmaceutics*, *291*(1–2), 183–188. https://doi.org/10.1016/j.ijpharm.2004.07.055

Li, Na, Wang, D., Sui, Z., Qi, X., Ji, L., Wang, X., & Yang, L. (2013). Development of an Improved Three-Dimensional *In Vitro* Intestinal Mucosa Model for Drug Absorption Evaluation. *Tissue Engineering Part C: Methods*, *19*(9), 708–719. https://doi.org/10.1089/ten.tec.2012.0463

Li, Nan, Lewis, P., Samuelson, D., Liboni, K., Neu, J., Lewis, P., … Liboni, K. (2004). Glutamine regulates Caco-2 cell tight junction proteins. *Am J Physiol Gastrointest Liver Physiol*, *287*, G726–G733.

Maier, T., Güell, M., & Serrano, L. (2009). Correlation of mRNA and protein in complex biological samples. *FEBS Letters*, *583*(24), 3966–3973. https://doi.org/10.1016/j.febslet.2009.10.036

Maltman, D. J., & Przyborski, S. A. (2010). Developments in three-dimensional cell culture technology aimed at improving the accuracy of in vitro analyses. *Biochemical Society Transactions*, *38*(4), 1072–1075. https://doi.org/10.1042/BST0381072

Matsusaki, M., Hikimoto, D., Nishiguchi, A., Kadowaki, K., Ohura, K., Imai, T., & Akash, M. (2015). 3D-fibroblast tissues constructed by a cell-coat technology enhance tight-junction formation of human colon epithelial cells. *Biochemical and Biophysical Research Communications*, *457*(3), 363–369. https://doi.org/10.1016/j.bbrc.2014.12.118

Miura, S., & Suzuki, A. (2017). Generation of Mouse and Human Organoid-Forming Intestinal Progenitor Cells by Direct Lineage Article Generation of Mouse and Human Organoid-Forming Intestinal Progenitor Cells by Direct Lineage Reprogramming. *Cell Stem Cell*, *21*, 456–471. https://doi.org/10.1016/j.stem.2017.08.020

Nakamura, T. (2018). Recent progress in organoid culture to model intestinal epithelial barrier functions. *International Immunology*, *31*(1), 13–21. https://doi.org/10.1093/intimm/dxy065

Nierode, G., Kwon, P. S., Dordick, J. S., & Kwon, S.-J. (2015). Cell-based Assay Design for High-Content Screening of Drug Candidates. *Journal of Microbiology and Biotechnology*, *26*(2), 213–225. https://doi.org/10.4014/jmb.1508.08007

Orlando, A., Linsalata, M., Notarnicola, M., Tutino, V., & Russo, F. (2014). Lactobacillus GG restoration of the gliadin induced epithelial barrier disruption: The role of cellular polyamines. *BMC Microbiology*, *14*(1), 1–12. https://doi.org/10.1186/1471-2180-14-19

Perdikis, D. A., Davies, R., Huravkov, A. Z., Nner, B. B. R. E., Etter, L., & N, M. D. B. (1998). Differential Effects of Mucosal pH on Human (Caco-2) Intestinal Epithelial Cell Motility , Proliferation , and Differentiation. *Digestive Diseases and Sciences*, *43*(7), 1537–1546.

Pereira, C., Araújo, F., Barrias, C. C., Granja, P. L., & Sarmento, B. (2015). Dissecting stromal-epithelial interactions in a 3D invitro cellularized intestinal model for permeability studies. *Biomaterials*, *56*, 36–45. https://doi.org/10.1016/j.biomaterials.2015.03.054

Richmond, C. A., & Breault, D. T. (2018). Move Over Caco-2 Cells: Human-Induced Organoids Meet Gut-on-a-Chip. *Cellular and Molecular Gastroenterology and Hepatology*, *5*(4), 634–635.

https://doi.org/10.1016/j.jcmgh.2018.01.016

Ross, M. H., Reith, E. J., Hubbel, W., Romrell, L. J., Kaye, G. I., & Kibiuk, L. V. (1995). *Histology: A Text and Atlas* (Third Edit). Lippincott Williams and Wilkins.

Spence, J. R., Mayhew, C. N., Rankin, S. A., Kuhar, M., Vallance, E., Tolle, K., … Wells, J. M. (2011). HHS Public Access. *Nature*, *470*(7332), 105–109. https://doi.org/10.1038/nature09691.Directed

Sun, H., Chow, E. C., Liu, S., Du, Y., & Pang, K. S. (2008). The Caco-2 cell monolayer: usefulness and limitations. *Expert Opinion on Drug Metabolism & Toxicology*, *4*(4), 395–411. https://doi.org/10.1517/17425255.4.4.395

Sung, J. H., Yu, J., Luo, D., Shuler, M. L., & March, J. C. (2011). Microscale 3-D hydrogel scaffold for biomimetic gastrointestinal (GI) tract model. *Lab Chip*, *11*(3), 389–392. https://doi.org/10.1039/C0LC00273A

Takenaka, T., Harada, N., Kuze, J., Chiba, M., Iwao, T., & Matsunaga, T. (2014). Human small intestinal epithelial cells differentiated from adult intestinal stem cells as a novel system for predicting oral drug absorption in humans. *Drug Metabolism and Disposition*, *42*(11), 1947–1954. https://doi.org/10.1124/dmd.114.059493

Tornavaca, O., Chia, M., Dufton, N., Almagro, L. O., Conway, D. E., Randi, A. M., … Balda, M. S. (2015). ZO-1 controls endothelial adherens junctions, cell-cell tension, angiogenesis, and barrier formation. *Journal of Cell Biology*, *208*(6), 821–838. https://doi.org/10.1083/jcb.201404140

Tunggal, J. A., Helfrich, I., Schmitz, A., Schwarz, H., Günzel, D., Fromm, M., … Niessen, C. M. (2005). E-cadherin is essential for in vivo epidermal barrier function by regulating tight junctions. *EMBO Journal*, *24*(6), 1146–1156. https://doi.org/10.1038/sj.emboj.7600605

Visco, V., Bava, F. A., D'Alessandro, F., Cavallini, M., Ziparo, V., & Torrisi, M. R. (2009). Human colon fibroblasts induce differentiation and proliferation of intestinal epithelial cells through the direct paracrine action of keratinocyte growth factor. *Journal of Cellular Physiology*, *220*(1), 204–213. https://doi.org/10.1002/jcp.21752

Waltenberger, B., Avula, B., Ganzera, M., Khan, I. A., Stuppner, H., & Khan, S. I. (2008). Transport of sennosides and sennidines from Cassia angustifolia and Cassia senna across Caco-2 monolayers - an in vitro model for intestinal absorption. *Phytomedicine*, *15*(5), 373–377. https://doi.org/10.1016/j.phymed.2007.03.008

Yamaguchi, H., Kojima, T., Ito, T., Kimura, Y., Imamura, M., Son, S., … Sawada, N. (2010). Transcriptional control of tight junction proteins via a protein kinase C signal pathway in human telomerase reverse transcriptase-transfected human pancreatic duct epithelial cells. *American Journal of Pathology*, *177*(2), 698–712. https://doi.org/10.2353/ajpath.2010.091226

Yamazaki, Y., Okawa, K., Yano, T., Tsukita, S., & Tsukita, S. (2008). Optimized Proteomic Analysis on Gels of Cell - Cell Adhering Junctional. *Biochemistry*, *47*(19), 5378–5386. https://doi.org/10.1021/bi8002567

Young, B., O'Dowd, G., & Philip, W. (2014). *Wheater's Functional Histology* (Sixth edit). Elsevier.

Yu, J., Peng, S., Luo, D., & March, J. C. (2012). In vitro 3D human small intestinal villous model for drug permeability determination. *Biotechnology and Bioengineering*, *109*(9), 2173–2178.

https://doi.org/10.1002/bit.24518

Zachos, N. C., Kovbasnjuk, O., Foulke-abel, J., In, J., Blutt, S. E., Jonge, H. R. De, & Estes, M. K. (2016). Human Enteroids / Colonoids and Intestinal Organoids Functionally Recapitulate and Pathophysiology *. *THE JOURNAL OF BIOLOGICAL CHEMISTRY*, *291*(8), 3759–3766. https://doi.org/10.1074/jbc.R114.635995

Zafarvahedian, E., & Ghahremani, M. H. (2018). Effect of Passage Number and Culture Time on the Expression and Activity of Insulin-Degrading Enzyme in Caco-2 Cells. *Iranian Biomedical Journal*, *22*(January), 70–75. https://doi.org/10.22034/ibj.22.1.70

Zhu, X., Wei, L., Bai, Y., Wu, S., & Han, S. (2017). FoxC1 promotes epithelial-mesenchymal transition through PBX1 dependent transactivation of ZEB2 in esophageal cancer. *American Journal of Cancer Research*, *7*(8), 1642–1653.

Ziegler, A., Gonzalez, L., & Blikslager, A. (2016). Large Animal Models: The Key to Translational Discovery in Digestive Disease Research. *Cmgh*, *2*(6), 716–724. https://doi.org/10.1016/j.jcmgh.2016.09.003

Zihni, C., Mills, C., Matter, K., & Balda, M. S. (2016). Tight junctions: From simple barriers to multifunctional molecular gates. *Nature Reviews Molecular Cell Biology*, *17*(9), 564–580. https://doi.org/10.1038/nrm.2016.80